OPTICAL ALGORITHMS FOR ASSESSMENT OF FLUORESCENCE SOURCES IN SEA WATERS

By

RUHUL AMIN

A dissertation submitted to the Graduate Faculty in Engineering in partial fulfillment of the requirements for the degree of Doctor of Philosophy

The City University of New York

2009

This manuscript has been read and accepted for the Graduate Faculty in Engineering in satisfaction of the dissertation requirement for the degree of Doctor of Philosophy.

Professor Samir Ahmed

Date

Chair of Examining Committee

Professor Mumtaz Kassir

Date

Executive Officer

Prof. Fred Moshary, Dept. of Electrical Engineering

Prof. Barry Gross, Dept. of Electrical Engineering

Prof. Alex Gilerson, Dept. of Electrical Engineering

Dr. Robert Stirbl, NASA Jet Propulsion Laboratory

Supervisory Committee

THE CITY UNIVERSITY OF NEW YORK

Abstract

OPTICAL ALGORITHMS FOR ASSESSMENT OF FLUORESCENCE SOURCES IN SEA WATERS

By

Ruhul Amin

Advisor: Professor Samir Ahmed

An optical algorithm, hereinafter called the Red Band Difference (RBD), is proposed and tested using sun induced chlorophyll fluorescence as the primary tool for the detection of relatively low backscattering phytoplankton blooms from space. The RBD technique is found to have potential for improving identification of blooms and their location compared to other algorithms. Since *Karenia brevis (K. brevis)* blooms are of great interest and have been commonly reported throughout the Gulf of Mexico, I also propose a *K. brevis* bloom classification algorithm, hereinafter called the *K. brevis* Bloom Index (KBBI). The KBBI technique is primarily based on the fact that total particulate backscattering associated with *K. brevis* bloom is different and much lower than that for non-*K. brevis* blooms. Since *K. brevis* bloomed water is known to have lower particulate backscattering than the non-*K. brevis* bloomed waters, the water-leaving radiance signal is much weaker for *K. brevis* blooms. As a consequence, the KBBI index becomes much larger for *K. brevis* blooms than for non-*K. brevis* blooms, thus permitting their distinction. The RBD and KBBI algorithms are capable of detecting relatively low

backscattering blooms and classifying *K. brevis* blooms respectively from Moderate Resolution Imaging Spectroradiometer (MODIS) and Medium Resolution Imaging Spectrometer (MERIS) ocean color measurements. To assess the efficacy of the detection and classification algorithms, simulations, including chlorophyll fluorescence (assuming 0.75% quantum yield) based on the *K. brevis* and non-*K. brevis* blooms conditions were performed and thresholds were determined. The approaches were applied to well documented blooms of *K. brevis* in the Gulf of Mexico and results were compared to other detection techniques such as Fluorescence Line Height (FLH). The application of the RBD was extended to test capabilities for detecting various toxic dinoflagellates blooms around the world. An analysis of impacts of the atmospheric corrections was performed on both of the algorithms.

To My Parents

Acknowledgments

I'm grateful to my advisor Professor Samir Ahmed for his patience and enthusiasm as an educator and scientist. I thank him for giving me the freedom to seek out my own path. I also extend my gratitude and appreciation to Professors Barry Gross, Fred Moshary and Dr. Jing Zhou for their valuable questions, suggestions, and comments which have strengthened many parts of this thesis research. In addition, I would like to thank Dr. Robert Stirbl from NASA JPL for serving in my supervisory committee. I'm also thankful to NASA, NOAA and ONR for providing funding for this research.

This research would not also have been possible without the support of my parents: Abdus Salam and Ayesha Begum, and my siblings: Rumena, Nadira, Nurul and Rubena. I would like to extend my sincerest appreciation to all my relatives for their prayers and thoughtfulness. Most of all I am thankful to Allah for allowing me to overcome many obstacles and making all these possible.

Table of Contents

List of Tables

Chapter 2

List of Figures

Chapter 2

List of Acronyms

Acronym	Description
CDOM	Colored Dissolved Organic Matter
Chl	Chlorophyll
ESA	European Space Agency
FLH	Fluorescence Line Height
HABs	Harmful Algal Blooms
KBBI	*Karenia brevis* Bloom Index
MERIS	Medium Resolution Imaging Spectrometer
MODIS	Moderate Resolution Imaging Spectroradiometer
NAP	Non-Algal Particles
NASA	National Aeronautics and Space Administration
NIR	Near Infrared
NOAA	National Oceanographic and Atmospheric Administration
RBD	Red Band Difference
RR	Reduced Resolution
SeaDAS	SeaWIFS data analysis system
SeaWiFS	Sea-viewing Wide Field-of-view Sensor
SNR	Signal to Noise Ratio
SWIR	Short Wave Infrared
TOA	Top of the Atmosphere
WFS	West Florida Shelf

CHAPTER 1 INTRODUCTION

Harmful algal blooms (HABs), also known as red tides due to the reddish discoloration of the sea surface, have been known to occur throughout human history. It is widely believed that one of the earliest potential documentation of the HABs is the Old Testament of the Bible [1]. However, in recent years HABs have become one of the serious environmental problems in the coastal areas on a global scale. The global nature of the problem has expanded both in its extent and its public perception over last several decades. Human activities and population increases have contributed to increase in various toxic and noxious algal species in the coastal regions worldwide [2, 3]. Eutrophication in estuaries and coastal waters are believed to be the major factor causing HABs [4, 5]. These HABs includes several classes of microalgae which includes diatoms, dinoflagellates, raphidophytes, cyanobacteria, prymnesiophytes, pelagophytes, and silicoflagellates [6]. However, dinoflagellates, the organisms that cause most of the red tides, have become the major concern for most of the coastal areas around the world. Probably their unique differences in adaptive ecologies are favoring their increasingly successful exploitation of coastal waters and global bloom expansion [7]. Marine HABs are usually caused by dinoflagellates and take place in warm regions or seasons and in places which are richer in nutrients such as coastal waters influenced by agricultural activity from inland regions [8]. Freshwater HABs, due to dinoflagellates, are much less widespread than in the sea [9]. Approximately 50% of all red tide forming species and 75% of all HAB species are dinoflagellates [10, 11].

Early detection and monitoring of HABs are very important for protecting public health, wild and farmed fish and shellfish, and endangered species such as marine mammals. Coastal business and tourism industry can also be vulnerable when dead fish wash up on shore, when surf activities creates tick layers of smelly foam on beaches, or when local sea food is suspected to be inedible. Furthermore, detection is also important because phytoplanktons play a major role in the global carbon cycle and blooms are responsible for much of the ocean carbon fixation. Since most of the world populations live close to the coast, any factor relating to oceans can affect significant number of people. As a result, rapid and reliable methods need to be established to detect and monitor bloom formation and transport to mitigate their harmful effects on the surrounding ecosystems and local communities.

Historically blooms have been observed by naked eyes because of the discoloration of the water. Now optical sensors can detect these changes in the color of the water and quantitatively tell us that possibly the water color has changed because of algae blooms. However, detection requires reliable optical techniques particularly for optically complex coastal waters. Optical techniques are very well suited for species such as dinoflagellates that aggregate to the surface for photosynthesis during the day. Their dense aggregations produce strong bio-optical signals which can be detected by the space borne and airborne optical sensors.

Many optical bloom detection algorithms have been developed based on in situ hyperspectral measurements. However, in situ detection algorithms have many limitations: they are labor intensive and suffer from practical limitations on achievable temporal and spatial resolutions, sampling maybe expensive and time consuming, and

detection may happen once the bloom has had an adverse effect. Hence, there has been a considerable interest on satellites since they can provide us with high spatial and temporal resolution, early blooms detection, guidance for in situ sampling, and can also show how a bloom changes with time either by growth or advection by physical processes. However, satellites are not without problems. Space borne optical sensors often suffer from blackouts of data due to the presence of clouds. Detection also has been hampered by the radiometers incapable of fully resolving the visible spectrum. Most of the ocean color sensors launched in last several decades have only few channels in the visible and mostly concentrated in the blue-green regions. For example, a sensor such as SeaWiFS is unable to identify the spectral signatures of the in-water particulate components such as phytoplankton, detritus, and minerals in the coastal waters [12]. It is impossible to spectrally separate the bloom signature from the sediment signature because their signatures overlap in the blue region of the spectrum used for ocean color determination [12]. However, with the launch of MODIS and MERIS with several bands in the red and NIR has enabled the scientific community to detect bloom more accurately than with the algorithms based on blue-green bands.

Even though many satellite bloom detection algorithms have been developed, it still remains a challenge to detect blooms in optically complex coastal waters. Algorithms based on blue-green bands don't work well in these waters because of the contaminations from the land, bottom, and atmospheric correction uncertainties. In recent years there has been an increasing interest in the red-NIR regions of the optical spectrums because of the (a) chlorophyll absorption peak, (b) chlorophyll fluorescence emission, (c) lower CDOM absorption, (d) less atmospheric corrections uncertainties than the blue-green regions and

(e) unique reflectance peak due to combined absorption of chlorophyll and sea water in this region. My interest particularly has been in the red region because of the chlorophyll fluorescence emission centered on 685nm. Developing algorithms based on the fluorescence signal would improve detection significantly because there is nothing else in the water that fluoresces in the red region. So, all the false bloom like features from CDOM plumes, sediment plumes, bottom reflectance, etc can more easily be removed. This would result in more accurate bloom detection and more precise bloom delineation.

The goal of this work is to develop detection algorithms for relatively low backscattering blooms and a classification algorithm for *Karenia brevis* blooms which blooms throughout the Gulf of Mexico particularly in Florida. The algorithms should be less sensitive to CDOM and atmospheric corrections uncertainties, and also should be applicable to multiple sensors so blackouts from cloud would be reduced. Furthermore, they should also minimize signal-to-noise (SNR) issues and eliminate errors due to retrieval algorithms.

References

1. Red Tide in Texas – An Explanation of the Phenomenon. Bulletin TAMU-G-86-006 C2. Marine Information Service, Sea Grant College Program, Texas A&M University, College Station, Texas. (1986)

2. G. M. Hallegraeff, In G. M. Hallegraeff, D. M. Anderson, and A. D. Cembella [eds.], Manual on harmful marine microalgae, UNESCO, (2003)

3. P. M. Glibert, D. M. Anderson, P. Gentien, E. Graneli, and K. G. Sellner, The global, complex phenomena of harmful algal blooms. Oceanography 18: 136–147, (2005)

4. A. J. McComb, Eutrophic Shallow Estuaries and Lagoons, 240 pp., CRC Press, Boca Raton, Fla. (1995)

5. T. J. Smayda, Novel and nuisance phytoplankton bloom in the sea: Evidence for global epidemic, in Toxic Marine Phytoplankton: Proceedings of the Fourth International Conference on Toxic Marine Phytoplankton, Held June 26 – 30 in Lund, Sweden, edited by E. Graneli et al., pp. 29–40, Elsevier Sci., New York, (1990)

6. J. H. Landsberg, The effects of harmful algal blooms on aquatic organisms. Reviews in Fisheries Science 10(2): 113-390, (2002)

7. T. J. Smayda, Turbulence, watermass stratification and harmful algal blooms: An alternative view and frontal zones as pelagic seed banks, Harmful algae 1:95-112, (2002)

8. C. V. Hoek, D. G. Mann and H. M. Jahns, Algae. *An introduction to phycology*, Cambridge University Press: 627pp. (1995)

9. S. Rodriguez, A. Coute, L. Tenhage and G. Mascarell, Peridiniopsis durandi sp. nova (Dinophyta), une nouvelle Dinophycee d'eau douce responsible de marees rouge, Algological Studies, 95: 15-29. (1999)

10. A. Sournia, Red-tide and toxic marine phytoplankton of the world ocean: An inquiry into biodiversity, in *Harmful Marine Algal Blooms*, edited by P. Lassus et al., pp. 103-112, Lavoisier, Paris. (1995)

11. T. J. Smayda, Harmful algal blooms: Their ecophysiology and general relevance to phytoplankton blooms in the sea, Limnol. Oceanogr., 42, 1137-1153, (1997)

12. S. C. Gallegos, X. Chen, and M. M. Crawford, A Report to TEXAS PARKS AND WILDLIFE, Remote Sensing Studies of the Gulf of Mexico – an effort in red tide detection, (September 2001)

CHAPTER 2 NOVEL OPTICAL TECHNIQUES FOR DETECTING AND CLASSIFYING TOXIC DINOFLAGELLATE KARENIA BREVIS BLOOMS USING SATELLITE IMAGERY

2.1 Introduction

Karenia brevis (*K. brevis*) blooms are of great interest and have been commonly reported throughout the Gulf of Mexico. In this chapter a detection technique is proposed for blooms with low backscatter characteristics, which we name the Red Band Difference (RBD) technique, coupled with a selective *K. brevis* bloom classification technique, which we name the *K. brevis* Bloom Index (KBBI). These techniques take advantage of the relatively high solar induced chlorophyll fluorescence and low backscattering of *K. brevis* blooms. The techniques are applied to the detection and classification of *K. brevis* blooms from Moderate Resolution Imaging Spectroradiometer (MODIS) ocean color measurements off the Gulf of Mexico. To assess the efficacy of the techniques for detection and classification, simulations, including chlorophyll fluorescence (assuming 0.75% quantum yield) based on *K. brevis* blooms and non-*K. brevis* blooms conditions were performed. These show that effective bloom detection from satellite measurements requires a threshold of RBD>0.15W/m²/μm/sr, corresponding to about $5 mg/m^3$ of chlorophyll. Blooms can be detected at lower concentration by lowering the RBD threshold but false positives may increase. The classification technique is found most effective for thresholds of RBD>0.15W/m²/μm/sr and KBBI>0.3*RBD. The techniques

were applied and shown to be effective for well documented blooms of *K. brevis* in the Gulf of Mexico and compared to other detection techniques, including FLH approaches.

2.2 Background

More than 40 species of toxic microalgae live in the Gulf of Mexico, but the most common is the toxic dinoflagellate *Karenia brevis* (*K. brevis*) formerly named *Gymnodinium breve* [1]. Although *K. brevis* blooms have been reported throughout the Gulf of Mexico, they are most frequent along the West Florida Shelf (WFS) where they occur nearly every year, usually between late fall and early spring but occasionally at other times of the year as well. *K. brevis* blooms have many negative impacts due to brevetoxin. This associated toxin causes death in fish, birds, and marine mammals [2]. It also can irritate human eyes and respiratory systems once it becomes airborne in sea spray [3, 4].

Many studies have been conducted to explore the optical characteristics of *K. brevis* [5-12]. Cannizzaro et al., (2008) [5] suggested that *K. brevis* blooms exhibit lower backscattering compared to other phytoplankton and this low backscattering efficiency has been related to its large size (20-40 μm) and low index of refraction (~1.05) [6]. Furthermore, backscattering of light in the ocean is typically dominated by submicron particles [13, 14], and thus the low backscatter associated with *K. brevis* blooms may also reflect lower associated concentration of submicron particles [15, 16]. Schofield et al., (2006) [8] suggested that the lower concentration of non-algal particles may be due to the toxicity of *K. brevis* cells which may directly inhibit bacterial growth and/or alter the organic material available for heterotrophic consumption.

Detecting and monitoring *K. brevis* blooms from field measurements is labor intensive and suffers from practical limitations on achievable temporal and spatial resolutions. Field measurements are typically made at discrete points and at discrete times, without much temporal continuity. To assist in the detection of blooms and the planning preparation of remedial measures to reduce health risks, etc., detection approaches with higher spatial and temporal resolutions are desirable. It is in this context that satellite Ocean Color sensors offer potential advantages for bloom detection and monitoring.

Stumpf et al., (2003) [17] proposed to use the magnitude of the difference between satellite chlorophyll concentration estimates and a background mean of chlorophyll estimates for the previous 0.5-2.5 months as an index for detecting bloom areas. At NOAA NESDIS CoastWatch, this method is now used operationally to alert for possible blooms in West Florida. Cannizzaro et al., (2008) [5] proposed another technique based on in situ data that uses the backscattering/chlorophyll ratio to discriminate between *K. brevis* and other blooms. They determined that *K. brevis* has lower backscatter characteristics than blooms of other diatoms and dinoflagellate species. Both of these methods are based on using the blue-green region of the spectrum. Unfortunately, blue-green reflectance ratio algorithms [18-20] have been found to perform poorly in coastal waters due to increased absorption of colored dissolved organic matter (CDOM), increased particle scattering, inaccurate atmospheric corrections and shallow bottom reflectance**.** Hu et al., (2005) [21] used Fluorescence Line Height (FLH) to detect and monitor *K. brevis* bloom on the WFS. However, our studies have shown

that FLH strongly overestimates the chlorophyll fluorescence signal under high elastic scattering conditions, resulting in false positives [22-24].

The objective of this study is to develop techniques for bloom detection and *K. brevis* bloom classification that are less sensitive to CDOM and atmospheric corrections, and apply them to satellite data to detect and classify *K. brevis* blooms in the Gulf of Mexico. In this study, we illustrate these approaches using the Moderate Resolution Imaging Spectroradiometer (MODIS) ocean color sensor which has several bands in the red and near-infrared (NIR) regions. This complements our previous study [25] where we used the Medium Resolution Imaging Spectrometer (MERIS) ocean color data.

In Section 2.3 that follows, the procedures for obtaining satellite imagery are briefly described. In Section 2.4, we present simulations of remote-sensing reflectance spectra ($R_{rs}(\lambda)$) for *K. brevis* and non-*K. brevis* blooms, introduce the proposed detection and classification techniques and discuss their backgrounds. Section 2.5 applies these techniques to satellite ocean color data and shows examples of detection, tracing, and classification of *K. brevis* blooms. We also compare the RBD detection and FLH techniques. Section 2.6 discusses the various advantages of the proposed techniques over other traditional techniques and examines possible false alarm conditions.

2.3 Satellite Data and Image Processing

MODIS imagery of WFS was obtained for different *K. brevis* blooms recorded in the literature dating from 2001 to 2006 from the NASA Ocean Color Website [26] and

processed to obtain the normalized water-leaving radiance ($nLw(\lambda)$) for visible and NIR bands, and FLH using SeaDAS version 5.0.3. The top of the atmosphere signals were corrected for the atmosphere using both the standard NIR [27] method and also the recently proposed [28] SWIR method for turbid coastal waters. The data was processed with a pixel size of 1km equal to the nominal pixel size of the sensor's ocean color bands.

2.4 Development of the Detection and Classification Techniques

2.4.1 Optical Modeling of K. brevis and non-K. brevis Blooms

Remote-sensing reflectance, $R_{rs}(\lambda)$ is defined as the ratio of water-leaving radiance to down welling irradiance, measured just above the sea surface. $R_{rs}(\lambda)$ can be approximately related to the subsurface remote-sensing reflectance, $r_{rs}(\lambda)$ [29] by:

$$R_{rs}(\lambda) = \frac{0.5 r_{rs}(\lambda)}{(1 - 1.5 r_{rs}(\lambda))} \tag{1}$$

where $r_{rs}(\lambda)$ for optically deep waters is given, according to [30] as:

$$r_{rs}(\lambda) = \left(0.084 + 0.17 \frac{b_b(\lambda)}{a(\lambda) + b_b(\lambda)}\right) \frac{b_b(\lambda)}{a(\lambda) + b_b(\lambda)} \tag{2}$$

The absorption ($a(\lambda)$) coefficients can be expressed as the sum of their individual components as

$$a(\lambda) = a_w(\lambda) + a_{ph}(\lambda) + a_{dg}(\lambda) \tag{3}$$

where $a_w(\lambda)$ is the absorption coefficient of water, obtained from [31], $a_{ph}(\lambda)$ is the absorption coefficients of phytoplankton, and $a_{dg}(\lambda)$ is the absorption coefficient which includes both CDOM (also known as gelbstoff) and detritus since they have similar spectral dependence. In the WFS area $a_{dg}(\lambda)$ is mostly contributed from CDOM (over 90%) [5] and we refer to it below as the CDOM absorption.

The relationship between phytoplankton $a_{ph}(\lambda)$ and chlorophyll [Chl] can be expressed by a power function

$$a_{ph}(\lambda) = A(\lambda)Chl^{B(\lambda)} \tag{4}$$

Here, values for $A(\lambda)$ and $B(\lambda)$ were taken from [5] for *K. brevis* bloom water containing greater than $10^4 cell/l$ (*K. brevis* bloom) and non-*K. brevis* bloom water containing less than $10^4 cell/l$ (non-*K. brevis* bloom).

Both CDOM and detritus absorb blue light strongly and absorption decreases with increasing wavelength as expressed by:

$$a_{dg}(\lambda) = a_{dg}(\lambda_\circ)\exp(-S_{dg}(\lambda - \lambda_\circ)) \tag{5}$$

where S_{dg} is the slope of absorption spectrum, and the reference wavelength $\lambda_\circ$ is 440nm. CDOM absorption at 440nm, $a_{dg}(440)$, was taken as ranging from 0 to $3\,m^{-1}$ for our simulation. Based on the documented field measurement data, S is in the range of 0.1 to 0.2 nm^{-1} with CDOM slope larger than that of detritus [5]. Here S_{dg} is taken as 0.014

nm^{-1}. Note here that $a_{dg}(440)$ does not correlate with chlorophyll concentration, as is the case for most optically complex coastal waters [32].

Similarly, the backscattering coefficient can be expanded as

$$b_b(\lambda) = b_{bw}(\lambda) + b_{bp}(\lambda) \tag{6}$$

where $b_{bw}(\lambda)$ is the backscatter coefficient of water obtained according to [33], and $b_{bp}(\lambda)$ is the total particulate backscatter coefficient.

Particulate backscattering spectra can be fitted to the form

$$b_{bp}(\lambda) = b_{bp}(550)(\frac{550}{\lambda})^{\gamma} \tag{7}$$

where γ is the Angstrom exponent that describes the spectral shape and can be modeled according to [5] by a modified relationship from [34] as :

$$\gamma = 0.1 + \frac{1.9}{(1 + Chl)} \tag{8}$$

Particulate backscattering at the reference wavelength for *K. brevis* and non-*K. brevis* blooms based on the cell concentrations of *K. brevis* was modeled according to [5] as follows:

$$b_{bp}(550) = 0.0051 Chl^{0.180} \text{ for } > 10^4 cells/l \text{ (}K.\ brevis\text{ blooms)} \tag{9a}$$

$$b_{bp}(550) = 0.0098 Chl^{0.977} \text{ for } < 10^4 cells/l \text{ (non-}K.\ brevis\text{ blooms)} \tag{9b}$$

Non-*K. brevis* blooms modeled in accordance with [5], which will be referred hereafter as non-*K. brevis*-1, were found to give high reflectance values for $Chl > 5mg/m^3$. They are represented by the total particulate backscattering model in Eq. 9b, which may be justified, since the non-*K. brevis* bloom model was developed from a dataset which was mostly dominated by diatoms, and in general, diatom blooms are associated with upwelling and freshwater inputs from rivers which contain large amounts of sediments [35].

However, to further investigate our classification technique, we use a second method which is based on a standard bio-optical model [32] to compute the particulate backscattering of non-*K. brevis* blooms while keeping the absorption term the same as for the non-*K. brevis*-1. This second category will be referred hereafter as the non-*K. brevis*-2. To model the non-*K. brevis*-2 blooms, we separated the particulate backscattering term $b_{bp}(\lambda)$ in Eq. 6 as follows:

$$b_{bp}(\lambda) = \tilde{b}_{b,nap} * b_{nap}(\lambda) + \tilde{b}_{b,ph} * b_{ph}(\lambda) \tag{10}$$

where $b_{nap}(\lambda)$ is the scattering coefficient of non-algal particles (NAP), $\tilde{b}_{b,nap}$ is the backscattering ratio of NAP, $b_{ph}(\lambda)$ is the scattering coefficient of phytoplankton, and $\tilde{b}_{b,ph}$ is the backscattering ratio of phytoplankton .

The NAP scattering is modeled by a power law function as follows:

$$b_{nap}(\lambda) = b_{nap}(550)(\frac{550}{\lambda})^{\gamma_2} \tag{11a}$$

where

$$b_{nap}(550) = b^{*}_{nap}(550) \cdot C_{nap} \tag{11b}$$

The specific scattering of NAP at 550nm, $b^{*}_{nap}(550)$, was assumed to be $0.5 m^2/g$, and $\gamma_2 = 1$. C_{nap} represents the concentration of NAP in mg/l. A constant backscattering ratio $\tilde{b}_{b,nap} = 2\%$ was assumed over the whole spectral band for the NAP [32]. We assumed a NAP concentration of $2 mg/l$ as typically co-existing with the non-*K. brevis* blooms. This should be a reasonably conservative assumption for NAP concentrations associated with diatom blooms (with increasing concentrations of NAP the separation between *K. brevis* blooms and non-*K. brevis* blooms becomes even more defined) [35].

Both high spectral resolution field measurements and simulations, which take into account the imaginary part of refractive index of algal cells, have shown that the phytoplankton attenuation decreases gradually with wavelength while its scattering spectrum is affected by absorption features due to anomalous dispersion [16, 36]. Following Lee [32], phytoplankton scattering is modeled as:

$$b_{ph}(\lambda) = c_{ph}(\lambda) - a_{ph}(\lambda) \tag{12}$$

where the attenuation spectrum $c_{ph}(\lambda)$ can be modeled as power law function [16, 37]:

$$c_{ph}(\lambda) = c_{ph}(550)\left(\frac{550}{\lambda}\right)^{\gamma_3} \tag{13a}$$

where

$$c_{ph}(550) = 0.3[chl]^{0.62} \tag{13b}$$

Here, $\gamma_3 = 1$ and the backscattering ratio $\tilde{b}_{b,ph} = 1\%$ were assumed constant over the whole spectral band for phytoplankton [32].

The total amount of fluorescence radiance just above the surface can be modeled according to [38] as follows:

$$LF = 0.54 \cdot \frac{1}{4\pi} \cdot \varphi \cdot \int_{400}^{700} \frac{a_{ph}(\lambda) \cdot E(\lambda,0)}{K(\lambda) + a_f} \cdot d\lambda \tag{14}$$

where the 0.54 factor accounts for the propagation of the fluorescence through the air-water interface, the $1/4\pi (sr^{-1})$ factor converts an isotropic fluorescence field to radiance, φ is the effective quantum yield of chlorophyll fluorescence which takes reabsorption into account [38] and was assumed to be 0.75%. This value falls on the upper side of the range determined for coastal waters [39]. $E(\lambda,0)$ is the downwelling scalar irradiance just below surface, and was taken from [40], $K(\lambda)$ is the attenuation coefficient in the fluorescence excitation zone, and a_f is the attenuation coefficient in the fluorescence emission zone. The fluorescence spectrum is modeled as $L_f(\lambda) = LF \cdot G(\lambda)$ where $G(\lambda)$ is Gaussian function centered at 685nm with a 25nm width. The absorption value at 685nm $a(685)$, was used to approximate the a_f term in the calculation. To estimate the diffuse attenuation coefficient, we use [41] to obtain:

$$K(\lambda) = 1.0547 \cdot \frac{a(\lambda) + b_b(\lambda)}{\cos(\theta_s)} \tag{15}$$

where θ_s is the solar zenith angle. $L_f(\lambda)$ is added to the elastic remote sensing reflectance obtained from Eq. (1) after normalizing with respect to the surface downwelling irradiance $E_d(\lambda)$.

From the above microphysical model, the construction of simulated remote sensing reflectances, $R_{rs}(\lambda)$, including both elastic and inelastic chlorophyll fluorescence components, can be performed. The first two simulated datasets were created for *K. brevis* cell concentrations, in accordance with [5], using the relationship for absorption of phytoplankton and particulate backscattering developed for *K. brevis* and non-*K. brevis* bloom waters. We also created a third dataset for non-*K. brevis* blooms using the non-*K. brevis*-2 model, where we separated backscattering of NAP and algal particles, and assumed NAP concentrations of $2mg/l$ to be always co-existing with the non-*K. brevis* blooms. We also created a fourth dataset for Case-1 (Open Ocean) waters in accordance with [42], in which Chl is the only input parameter:

$$b_{bp}(\lambda) = [0.002 + 0.02(0.5 - 0.25\log_{10} Chl)\frac{550}{\lambda}] \cdot 0.3Chl^{0.62} \tag{16}$$

$$a_{ph}(\lambda) = 0.06Chl^{0.65} \tag{17}$$

$$a_{dg}(\lambda) = 0.2[a_w(440) + 0.06Chl^{0.65}]\exp(-0.014(\lambda - 440)) \tag{18}$$

Since these waters normally have a pronounced fluorescence component, it is important to distinguish them from waters with *K. brevis* blooms. Finally, the $nLw(\lambda)$ was derived by multiplying the $R_{rs}(\lambda)$ by the extraterrestrial solar constant in accordance with [43].

2.4.2 Background of Detection and Classification Algorithms

The essence of our approach is that the water-leaving radiance spectra of *K. brevis* and non-*K. brevis* blooms have distinctive features in the red region of the spectrum which can be used to detect and classify *K. brevis* blooms. The red spectral region is particularly attractive since it is less contaminated by CDOM and bottom reflectance, and is less susceptible to atmospheric correction difficulties than the blue-green region. As a consequence, uncertainties in bloom detection algorithms are reduced if this spectral region is used instead of the blue-green region. The distinguishing optical features of *K. brevis* and non-*K. brevis* blooms are demonstrated in Fig. 1. The simulated elastic reflectance, $R_{rs}(\lambda)$ without chlorophyll fluorescence (green spectra) shows a trough around 675nm due to the absorption of chlorophyll for both types of blooms. When a fluorescence signal is included in the simulation (red spectra), the trough of the *K. brevis* bloom shifts toward shorter wavelengths around 667nm, or less, depending on chlorophyll concentrations and its quantum yield while the trough of non-*K. brevis* bloom remains around 675nm. The shift in the *K. brevis* spectra is due to the fact that *K. brevis* exhibit lower backscattering efficiency, so the fluorescence signal dominates the red reflectance spectral region. Because of the overlap of the phytoplankton absorption and chlorophyll fluorescence emission, when fluorescence is a significant portion of the reflectance signal, the trough in the red region shifts towards shorter wavelengths, which is the case for *K. brevis*. On the other hand, non-*K. brevis* blooms (mostly dominated by diatoms) have higher backscattering efficiency, so reflection is dominated by the elastic backscattering component, therefore the fluorescence signal represents only a very small portion of the total reflectance, and is too weak a contributor (compared to the

backscatter signal) to result in any significant spectral changes. As a consequence, the trough of non-*K. brevis* blooms reflectance remains around the maximum of the phytoplankton absorption spectra (Fig. 1).

2.4.3 Detection Algorithm

Based on the above observations showing that the minimum of $R_{rs}(\lambda)$ can shift from the phytoplankton absorption maximum, around 678nm, to shorter wavelengths, around 667nm, with significant chlorophyll fluorescence contributions in the red spectral region, we can define a bloom detection technique which we identify simply as the Red Band Difference (RBD) as follows:

$$RBD = nLw(678) - nLw(667) \tag{19}$$

Simulation shows that the positive RBD values ($>1 mg/m^3$ of Chlorophyll) are primarily due to the fluorescence signal which correlates strongly with the chlorophyll concentration of the *K. brevis*. Because of this strong correlation, it may be possible to quantify *K. brevis* and other blooms with similar characteristics in terms of the chlorophyll concentrations more accurately than the standard reflectance band ratio algorithms [18-20] by developing some empirical relationship between the RBD and the bloom (*K. brevis* and other low backscattering blooms) chlorophyll using in situ data.

Since the RBD technique may also be able to detect blooms of other species, particularly the low backscattering ones, we further propose, below, an additional *K. brevis* bloom classification technique, KBBI, to discriminate *K. brevis* blooms from other

blooms and bloom like features such as CDOM plumes, sediment plumes and bottom reflectance.

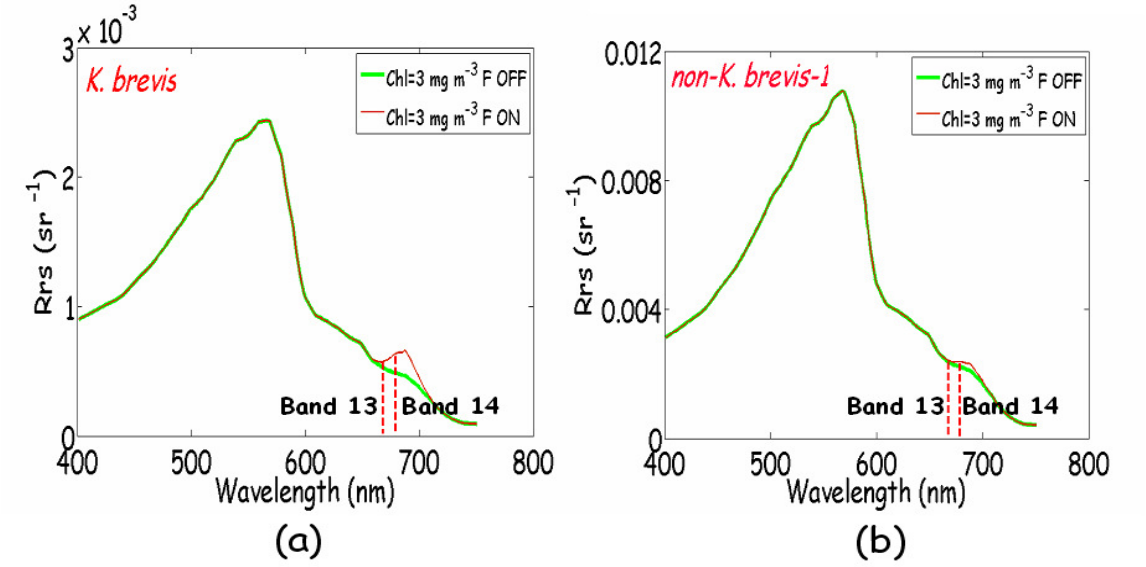

Fig. 1. Modeled remote sensing reflectance spectra for *K. brevis* cell concentrations (a) greater than $10^4 cells/l$ (*K. brevis* bloom) and (b) less than $10^4 cells/l$ (non-*K. brevis*-1 bloom) for the $Chl = 3mg/m^3$ and $a_{dg}(440) = 0.25m^{-1}$. The solid green spectra are when chlorophyll fluorescence is excluded ("F OFF") from the simulation and solid red spectra are when fluorescence is included ("F ON") in the simulation assuming 0.75% quantum yield. Band 13 and 14 are MODIS bands centered at 667nm and 678nm respectively.

2.4.4 Classification Algorithm

We define the *K. brevis* bloom index (KBBI) as follows:

$$KBBI = \frac{nLw(678) - nLw(667)}{nLw(678) + nLw(667)} \tag{20}$$

The KBBI technique is primarily based on the fact that total particulate backscattering associated with *K. brevis* is different from that for non-*K. brevis* blooms. Since *K. brevis* bloom water is known to have lower total particulate backscattering [5- 8] than the non-*K. brevis* bloom waters, the water-leaving radiance signal is much weaker for *K. brevis* blooms than for the non-*K. brevis* blooms since it is largely proportional to backscattering. As a consequence, the denominator of Eq.20, which is just the sum of the two MODIS red bands (band 13 and band 14), becomes much larger for non-*K. brevis* blooms than for *K. brevis* blooms. Furthermore, the numerator of Eq.20, which is the RBD, is much more pronounced for *K. brevis* blooms than the non-*K. brevis* blooms. Therefore, the KBBI values for *K. brevis* are usually higher than that of non-*K. brevis,* thus permitting the separation.

2.5 Results

2.5.1 Detection of K. brevis Blooms

Using the RBD detection technique, we detected various *K. brevis* blooms in the Gulf of Mexico. Fig. 2 demonstrates two examples of *K. brevis* bloom detection on the WFS. The RBD image in Fig. 2a is created for MODIS (Terra) image 17 Sep 2001 [44, 48] while the RBD image in Fig. 2b is created for MODIS (Aqua) image 21 Jan 2005 [45]. At the same time their corresponding KBBI images are displayed in Fig. 2c, d and will be discussed further below. To further investigate the potential of the RBD technique, the *K. brevis* bloom that took place between October and December 2004 on WFS, was traced over several weeks period. According to [21] the bloom by mid-late

November contained high concentrations ($>10^5 cells/l$) of *K. brevis* cells and caused higher mortalities of fish and dolphins. Fig. 3 shows an example of bloom tracing where the bloom drifted southward and expanded to form a large curved patch around 25.5 ºN 82.5 ºW from early November to mid December, and in subsequent weeks the bloom moved further to the south and formed a continuous band parallel to the Florida Keys [21]. These results are found to match reasonably well with cell count data from in-situ measurements, obtained from [46] which were overlaid on top of images in Figs 2, 3 and 6 with H (black), L (red), and N (green) representing $>10^6 cells/l$, $<10^6 cells/l$ and not present respectively.

The RBD images created from MODIS data often shows striping at the end of each scan line due to the variations in detector response. Also significant noise was noticed at the cloud edge pixels due to scattering from clouds affecting nearby pixels. However, both the striping and the noise at the cloud edge (which are retained in all figures) have significantly different appearances from bloom patches and can be easily distinguished in observation. Our analysis of the satellite data shows that using a threshold of RBD$>0.15 W/m^2/\mu m/sr$ readily identifies legitimate bloom areas.

The modeled RBD values as a function of Chl for various types of blooms with $a_{dg}(440)$ fixed at $0.25 m^{-1}$ are demonstrated in Fig. 4a. This simulation shows that to reach the RBD threshold values stated above, may require chlorophyll as high as $5 mg/m^3$ with the assumed 0.75% fluorescence quantum yield. By using a $Chl>1 mg/m^3$ to define a blooming condition [21], the simulation results show that an RBD threshold value lower than $0.15 W/m^2/\mu m/sr$ is possible. However this lower threshold will increase false

positives from satellite data analysis. Thus a compromise between simulations and satellite data analysis was made to arrive at the $0.15W/m^2/\mu m/sr$ RBD threshold.

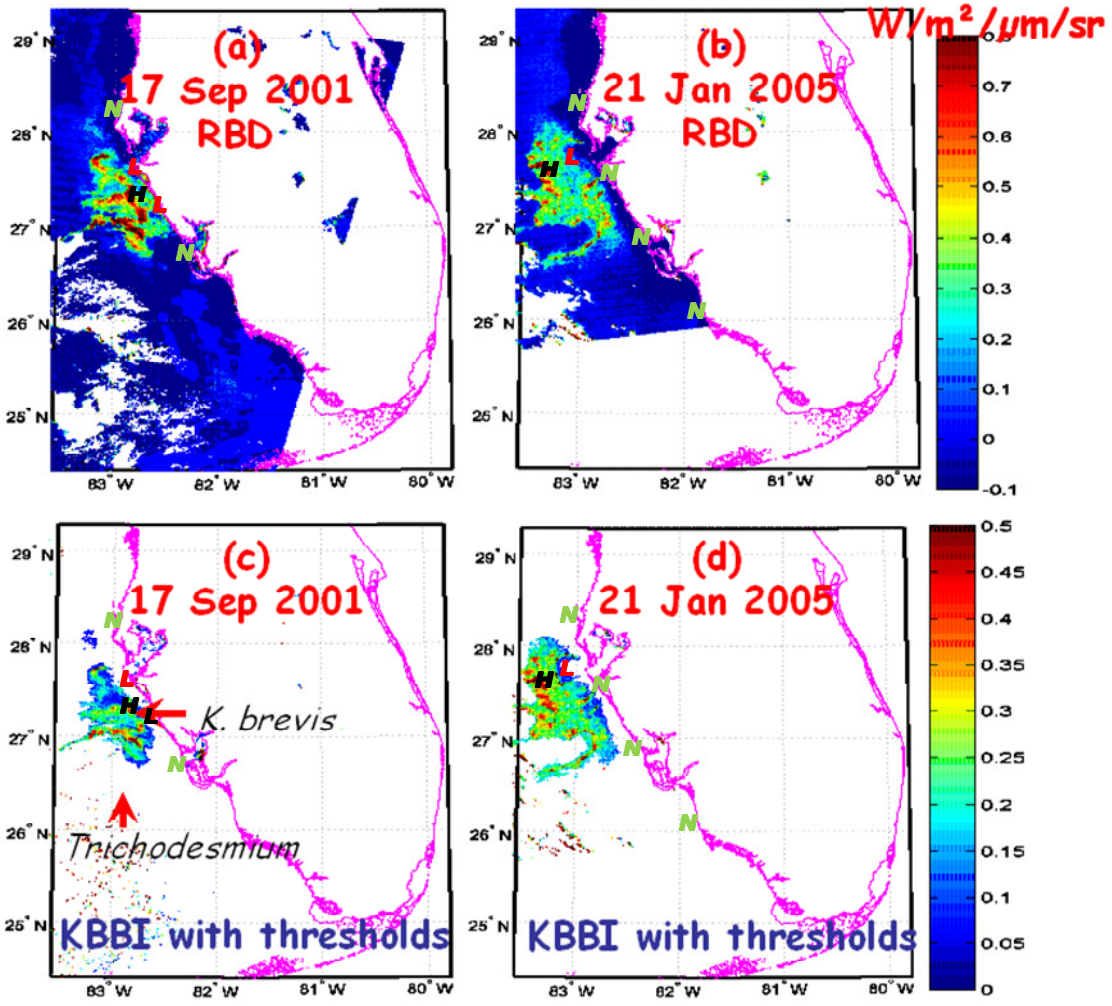

Fig. 2. *K. brevis* blooms detected using the RBD technique on the WFS on (a) 17 Sep 2001, and (b) 21 Jan 2005. These blooms are classified as *K. brevis* blooms using the KBBI classification technique with appropriate thresholds applied on (c) 17 Sep 2001 and (d) 21 Jan 2005. The 17 Sep 2001 image is an example when *K. brevis* and *Trichodesmium* blooms were co-occurring spatially but only *K. brevis* bloom is detected. Cell concentration sampling data obtained from [46] are shown as H (black), L (red), and N (green) representing $>10^6 cells/l$, $<10^6 cells/l$ and not present respectively.

The distinction between *K. brevis* and the non-*K. brevis*-1 can be clearly seen in Fig. 4a. However the *K. brevis* and Case-1 waters both give nearly the same RBD responses for *Chl* ranging from 1 to $100\,mg/m^3$. Even the non-*K. brevis*-2 model gives similar RBD values especially when *Chl* goes beyond 20 mg/m^3. The high backscattering level for non- *K. brevis*-1 leads to a dominant elastic signal in the reflectance at the red spectral region with a minima around 675nm, even at high *Chl* . As a result the reflectance signal in the 678nm is lower than that at 667nm, which results in negative RBD values. On the other hand, the backscattering level for non-*K. brevis*-2 and Case-1 waters is not high enough to be distinguished from the *K. brevis* cases. Therefore the RBD itself is not sufficient to identify whether a bloom is produced by *K. brevis* or other species although it may discriminate between *K. brevis* and non-*K. brevis*-1 bloom waters (assuming backscattering relationship developed by [5] represents true non-*K. brevis* blooms backscattering and true fluorescence quantum yield is close to the assumed value). It is also reasonable to expect that the RBD technique maybe used to detect blooms of other species as well that have somewhat similar optical characteristics as the *K. brevis* blooms.

As discussed and shown in Fig. 4a, the RBD technique alone cannot differentiate between *K. brevis* bloom waters and Case-1 waters with high concentration of chlorophyll (even though it might be argued that it is very unlikely to have high concentrations of chlorophyll ($>5mg/m^3$) in Case-1 waters unless if there is some sort of algal bloom present). To deal with the ambiguity that the RBD technique alone is not sufficient to distinguish *K. brevis* blooms, application of the KBBI technique is proposed for selective classification of *K. brevis* blooms, and is discussed next.

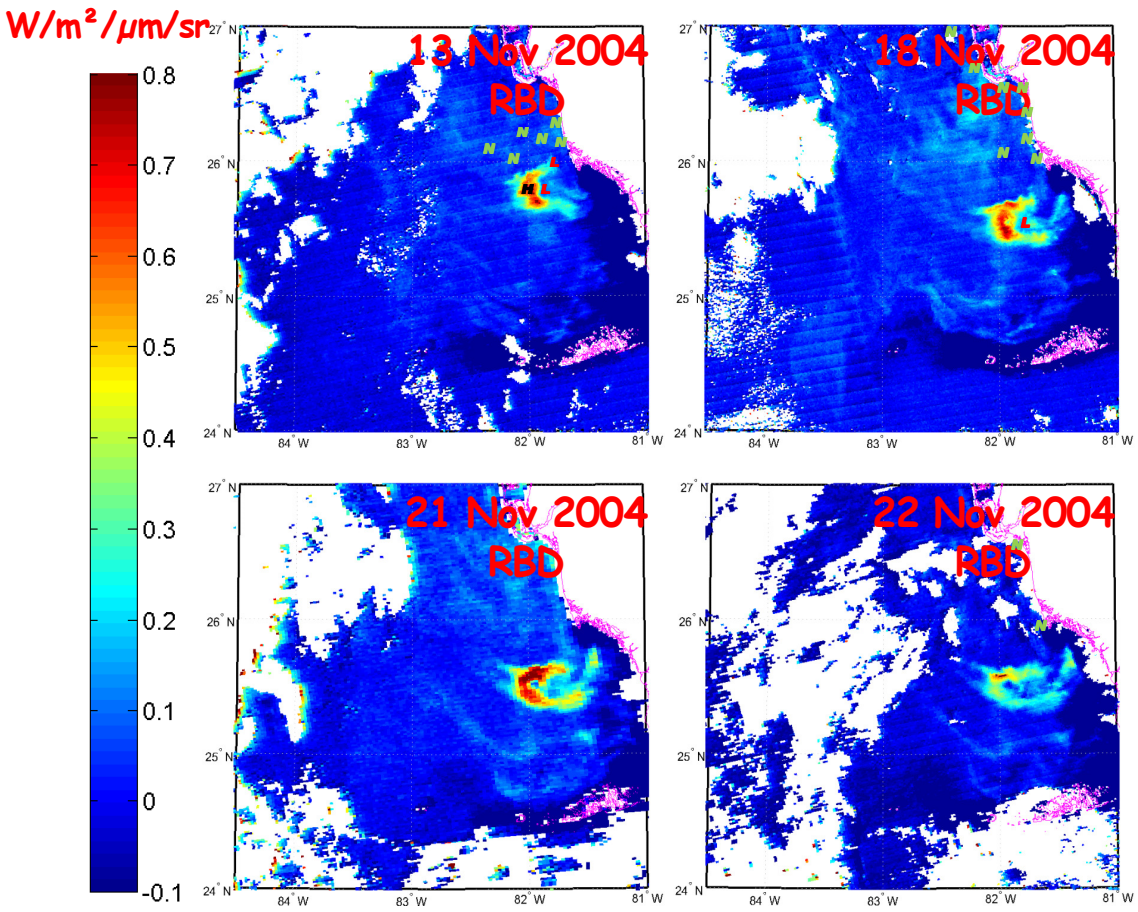

Fig. 3. MODIS RBD image series show the progression of a *K. brevis* bloom. Land and cloud pixels are shown in white. The bright pixels next to the cloud are noise from clouds. Cell concentration sampling data obtained from [46] are shown as H (black), L (red), and N (green) representing $> 10^6 cells/l$, $< 10^6 cells/l$ and not present respectively.

2.5.2 Classification of K. brevis Blooms using KBBI

In Fig, 4b, KBBI values are plotted as a function of *Chl* . As can be seen, there are higher KBBI values for *K. brevis* blooms than for other species with similar *Chl*, which opens up possibilities for distinguishing between *K. brevis* and other species.

Therefore, to achieve effective separation of the *K. brevis* blooms from other blooms, we need to combine the RBD and KBBI techniques together. This approach is discussed below for a variety of coastal water conditions.

Since coastal waters are often impacted by CDOM absorption (causing algorithms using simple blue-green reflectance ratios to perform poorly), it is important that we explore the sensitivity of our proposed indices to CDOM impacts and other water properties typically expected in turbid waters. To explore these issues, the simulation was performed for two extreme values: $a_{dg}(440) = 0$ and $3m^{-1}$ respectively, while keeping all other parameters constant as shown in Fig.5. Although these extreme values may not reflect conditions that naturally occur on the WFS, they at least provide a general idea of the boundaries for RBD and KBBI values due to CDOM absorption, which suffices for our detection and classification purpose. Increasing concentrations of CDOM in the water column are seen to result in a reduction in fluorescence signal. This cause the RBD and KBBI values to decrease slightly, given the prominence of chlorophyll fluorescence in these techniques. Since CDOM is assumed to have zero scatter, this decrease can be attributed to the absorption effects of CDOM, reducing the availability of photons in the chlorophyll fluorescence excitation waveband, and the consequent reduction of the fluorescence signal. The discrimination of *K. brevis* blooms from other blooms can also be observed in Fig. 5 where slopes for *K.Brevis* lines are greater than that for all other cases under consideration. The slopes are lower at $a_{dg}(440) = 0$ (Fig. 5: 1a & 2a) than that at $3m^{-1}$ (Fig. 5: 1b & 2b). This is due to the normalization factor in the KBBI technique, which increases with the decrease of a_{dg}.

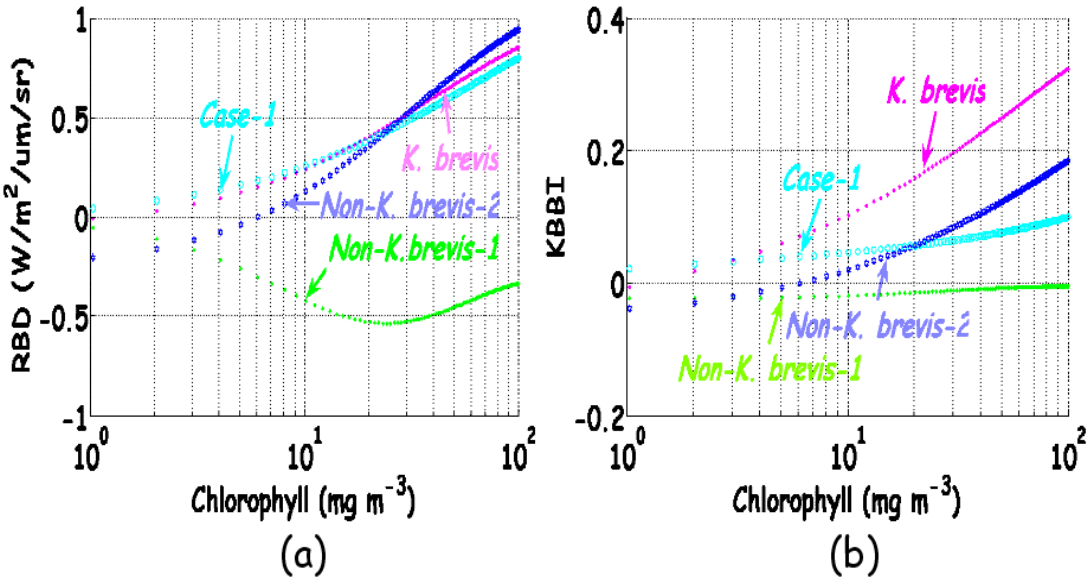

Fig. 4. Modeled (a) RBD ($W/m^2/\mu m/sr$) and (b) KBBI values as a function of chlorophyll concentrations generated for *K. brevis* blooms (magenta), non-*K. brevis*-1 (green), non-*K. brevis*-2 (purple), and Case-1 (cyan) waters. $a_{dg}(440) = 0.25m^{-1}$

To further examine the efficacy of the classification technique over a wide range of water compositions, we used non-*K. brevis*-2 simulated data along with the case-1 simulated data as tests for separating *K. brevis* blooms from other types of water and blooms. The dotted points in Fig. 5 are taken from MODIS Aqua sensor images which contains data from the regions between (25.5ºN - 25.9ºN) and (81.9ºW - 82.3ºW) for 13 Nov 2004 (cyan) image and (25.39ºN - 25.5ºN) and (81.683ºW - 82.266ºW) for the 18 Nov 2004 (yellow) image. These regions included *K. brevis* blooms as well as neighboring pixels which may have contained *K. brevis* cells, but in low concentrations. The *K. brevis* values obtained from satellite data in Fig. 5 show slightly higher KBBI values than those from the simulated *K. brevis* data. This is probably due to the

uncertainties caused by data retrieval using standard NIR atmospheric correction algorithm [47].

After analyzing simulation data coupled with the satellite data, we obtained the following thresholds for *K. brevis* bloom classification.

(1) $RBD > 0.15$ W/m²/μm/sr, and

(2) $KBBI > 0.3*RBD$

However, since these thresholds were derived assuming a chlorophyll fluorescence quantum yield of 0.75% and only the central waveband of each channel was used rather than the weighted average of the bandwidth, these values need to be further refined with in situ data.

To broaden the examination, twenty cloud free *K. brevis* bloom images from seven different bloom events (5 from WFS and 1 from the Texas Coast) were taken from literature dating between 2001 and 2006. The results are summarized in Table 1. All twenty RBD images detect the bloom locations documented in the literature at least as well as other techniques such as chlorophyll anomaly and FLH. Furthermore in several occasions RBD removes false positive given by FLH imagery due to high scattering of NAP. Three of the KBBI images without thresholds gave false positives in the areas where RBD didn't detect any bloom. This is probably due to the contamination from thin clouds or atmospheric uncertainties. However, when proposed thresholds were applied to create *K. brevis* classification images, those false positives disappeared.

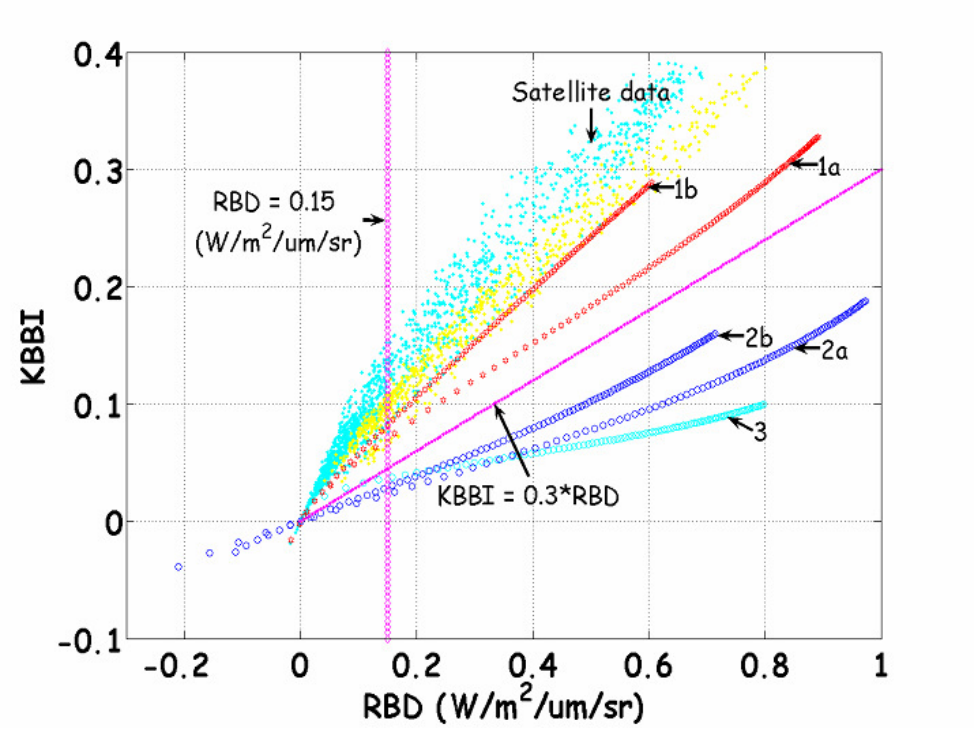

Fig. 5. Relationship between modeled RBD ($W/m^2/\mu m/sr$) and KBBI values for *K. brevis* blooms with $a_{dg}(440)=0m^{-1}$ (red, "1a") and $a_{dg}(440)=3m^{-1}$ (red, "1b"), non-*K. brevis*-2 with $a_{dg}(440)=0m^{-1}$ (blue, "2a") and $a_{dg}(440)=3m^{-1}$ (blue, "2b"), and Case-1 (cyan, "3") waters. Dotted points represent MODIS (Aqua) data corrected using the NIR atmospheric correction algorithm and collected on 13 Nov 2004 (25.5ºN – 25..9ºN, 81.9ºW - 82.3ºW) (cyan) and 18 Nov 2004 (25.39ºN - 25.5ºN, 81.683ºW - 82.266ºW) (yellow). Also shown is a RBD threshold line (magenta) equal to $0.15W/m^2/\mu m/sr$ and the relationship KBBI=0.3*RBD (magenta). The satellite data includes *K. brevis* bloomed water and also closed by waters which may contain *K. brevis* cells but in low concentrations.

Table 1. Studied MODIS bloom images. Detected and classified blooms with RBD and KBBI are shown with "√" while the symbol "√/×" under KBBI represents images where RBD and KBBI agreed in the bloomed area but KBBI gave false positives close to the coast where RBD didn't detect any bloom. The Chlorophyll Anomaly [17] method is referred as ChlA.

Bloom events	Date	Regions in the Gulf of Mexico	RBD	KBBI	Other techniques	References
1	09/17/01	WFS	√	√	ChlA	[48 , 44]
2	02/04/02	WFS	√	√	Enhanced RGB	[49]
	02/17/02	WFS	√	√	True-color	[50]
3	10/09/03	WFS	√	√/×	Enhanced RGB	[49]
	10/19/03	WFS	√	√	Enhanced RGB / FLH	[49]
4	10/30/04	WFS	√	√	FLH	[21]
	11/07/04	WFS	√	√	FLH	[21]
	11/13/04	WFS	√	√/×	ChlA / FLH	[51, 21]
	11/18/04	WFS	√	√	ChlA / FLH	[51, 21]
	11/21/04	WFS	√	√/×	FLH	[21]
	11/22/04	WFS	√	√	ChlA / FLH	[51, 21]
	12/04/04	WFS	√	√	FLH	[21]
	12/13/04	WFS	√	√	ChlA / FLH	[51, 21]
5	01/21/05	WFS	√	√	ChlA / FLH	[51, 45]
	02/08/05	WFS	√	√	FLH	[45]
	02/09/05	WFS	√	√	FLH	[45]
6	09/26/05	WFS	√	√	FLH	[52]
	09/27/05	WFS	√	√	FLH	[52]
	09/29/05	WFS	√	√	ChlA / FLH	[51, 52]
7	10/06/06	Texas	√	√	True-color	[53]

Fig. 2c & 2d are for the same conditions as shown in Fig. 2a & 2b respectively, and apply the proposed threshold conditions for both RBD and KBBI. Fig. 2a & 2c show

an example where *K. brevis* and *Trichodesmium* blooms were both known to co-exist (identified by red arrows in 2a) on the WFS [44]. As can be seen in Fig. 2c, the proposed *K. brevis* classification technique only extracts the *K. brevis* bloomed area and ignores the *Trichodesmium* bloomed area. This distinction is primarily due to the relative backscattering characteristic of *K. brevis* and *Trichodesmium* blooms. *Trichodesmium* blooms are well known to backscatter strongly [54]. Whenever backscattering is strong, the KBBI values are negative or very close to zero, so these blooms are not detected.

2.5.3 Comparison between RBD and FLH

Although FLH can sometimes be used to detect blooms [21], it breaks down in highly scattering waters, where high red peak values are primarily due to contributions from elastic scattering modulated by chlorophyll absorption rather than the fluorescence, thus falsely indicating possible blooms. Thus, as the concentration of NAP increases, radiance generally raises as well, and the fluorescence peak becomes a less prominent component of increased total signal.

In contrast, the RBD technique is found to easily differentiate between the two effects, giving positive values in truly bloomed waters and negative values in highly scattering waters. The performance of MODIS FLH calculations can be assessed for turbid waters by comparing FLH values with true fluorescence values at 685nm. Simulations show that the true fluorescence signal at 685 nm decreases as a fraction of the total signal for increasing concentration of NAP. However, MODIS FLH shows an opposite trend and a significant overestimation of the true fluorescence signal. The most

dramatic effect is the overestimation of true fluorescence when chlorophyll is low and NAP increases. Similar results were found in [23, 24, 55]. Tomlinson, et al., (2008) [56] also pointed out that FLH was unreliable in the area surrounding the Florida Keys; giving elevated values in all of the images they examined which is in agreement with our analysis of satellite imagery for this region. Clearly, the FLH algorithm can breakdown for turbid waters and if used for *K. brevis* bloom detection would also flag pixels with turbid waters as possible *K. brevis* blooms. On the other hand, the RBD technique only detects true blooms and gives negative or near zero values for highly scattering waters, so does the KBBI classification technique. This is more clearly illustrated in Fig. 6, which shows MODIS Aqua bloom images from November 13, 2004 on the WFS. To examine whether the intense regions in the FLH image are due to blooms or highly scattering waters, we took three spectra from the three supposedly bloomed regions (bloomed, turbid-1, and turbid-2) as indicated by FLH (Fig. 6a) and plotted the resultant spectra in Fig. 6c. We see that the true *K. brevis* bloom spectrum (Fig. 6c; red) differs significantly from the other two spectra particularly in the blue-green region of the optical spectrum where they both give significantly higher values than the bloomed spectra. So the spectra (Fig. 6c; green and blue) taken from turbid-1 and turbid-2 region of Fig. 6a are due to highly scattering waters, and not characteristic of *K. brevis*. Furthermore, it is seen that the signals in the red bands of these spectra are also significantly different where the *K. brevis* bloom spectra (Fig. 6c; red) has a positive slope from 667nm band to 678nm band while other two have negative slopes. The slope is negative only when water is highly scattering. Therefore, the region in Fig. 6a indicated by turbid-1 and turbid-2 must be

due to highly scattering waters and not *K. brevis* blooms. Those false blooms signals based on FLH clearly disappear in the RBD image (Fig. 6b).

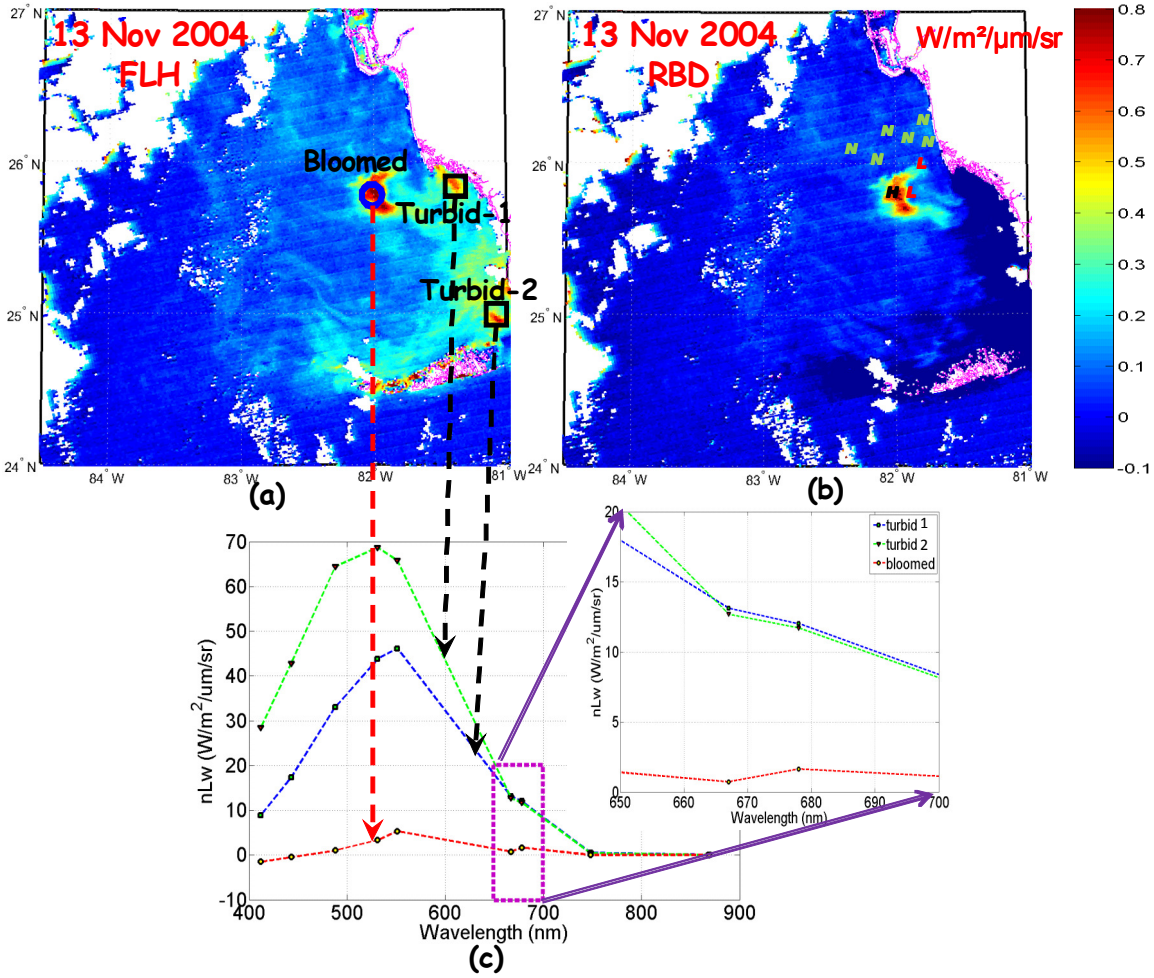

Fig. 6. MODIS (Aqua) bloom image from 13 November 2004 for the WFS (a) FLH ($W/m^2/\mu m/sr$) image, (b) RBD ($W/m^2/\mu m/sr$) image and (c) Normalized-water leaving radiance spectra taken from the bloomed and turbid waters indicated by "circle" and "squares" respectively in the FLH image. Cell concentration sampling data obtained from [46] are shown as H (black), L (red), and N (green) representing $>10^6 cells/l$, $<10^6 cells/l$ and not present respectively.

2.6 Discussion

Chlorophyll retrieval from reflectance spectra remains a challenge in coastal waters, and may even be an impossible task in some cases, particularly when CDOM concentrations are high [57]. MODIS red bands 13 and 14 were designed with high signal-to-noise ratios to avoid various problems including CDOM for retrievals of fluorescence, and hence chlorophyll. However, in highly scattering waters, typical in coastal areas, the fluorescence component represents a small portion of the total reflectance signal, and FLH algorithms erroneously extract a combined elastic scattering and fluorescence signal, rather than the much smaller fluorescence signal.

When low concentrations of NAP and low scattering conditions exist, the red spectral region becomes chlorophyll fluorescence dominated. Furthermore, this spectral region is less affected by CDOM, shallow bottom, and even atmospheric correction uncertainties than the blue-green region. Since the *K. brevis* bloom is known to have a much lower backscattering efficiency, the red signals from *K. brevis* blooms are usually largely dominated by the *K. brevis* chlorophyll fluorescence. The RBD technique takes advantage of this fluorescence dominated signal to detect these types of blooms. Normalization then makes it possible for the KBBI technique to discriminate *K. brevis* from non-*K. brevis* blooms. When applied to existing satellite imagery, we find that applying the thresholds proposed in section 2.5.2, the *K. brevis* blooms were detected and classified successfully over a wide time span in the WFS. This included the bloom event of 2004 on the WFS which was successfully tracked for several weeks.

The techniques developed in this study for detecting and classifying *K. brevis* blooms using satellite ocean color measurements appear to have advantages over other techniques developed using blue-green bands [5, 17] and even red-NIR bands such as FLH. Recently it has been suggested in [56] that future studies should examine the use of a FLH anomaly as a potential replacement to the chlorophyll anomaly method. However, it can be seen from our work here and previously [22-24] that any significant NAP scattering gives red peaks where the main contribution is from elastic reflection modulated by the confluence of chlorophyll and water absorption rather than from fluorescence, which results in false identification of fluorescence peaks in NAP rich waters. In contrast, the RBD technique eliminates association of an elastic peak with a bloom, by giving a negative value when these circumstances occur. Both RBD and KBBI techniques are much less affected by uncertainties in atmospheric correction algorithms. This is particularly true for the RBD detection technique because it uses band differences of two spectrally close lying bands, for which the atmospheric impact is little changed, and more importantly because differences rather than ratios are used. Thus analysis shows that the detection technique gives nearly the same result with different atmospheric correction algorithms. Classification of *K. brevis* bloom from *Trichodesmium* bloom is also possible if *K. brevis* blooms spatially co-exist with high-backscattering *Trichodesmium* blooms [44, 54] since KBBI gives negative or nearly zero values for highly backscattering blooms. Furthermore, Hu et al., (2005) [21] suggested that using FLH data along with knowledge of local water and ERGB composite imagery, an operator may make it possible to identify whether a feature is shallow bottom, resuspended sediment, a phytoplankton bloom, or a CDOM-rich plume. However, the

RBD and KBBI techniques seem to be capable, possibly with some additional tuning, of eliminating or at least minimizing most of these issues.

We also would point out that the RBD or the KBBI imagery generated from MODIS often shows striping due to the variation in the response among detectors and significant noise near the cloud edges which is consistence with the previous studies of FLH [21]. However, if all threshold conditions are used simultaneously, cloud edge noise or striping effects should not be a problem. Furthermore, cloud edge noise can be flagged out by flagging out cloud edge pixels and the striping is very easily distinguishable using spatial pattern techniques and can be flagged out as well. Additional errors in the classification technique may be introduced due to normalization in highly absorbing waters, or from inappropriate atmospheric correction algorithms, which may affect the KBBI index somewhat. However, since the RBD indicator used at the same time would not give false signal in such waters, these problems can be avoided by checking agreement between the RBD and KBBI imagery or using the proper thresholds.

2.7 RBD & KBBI Assessment

We have introduced two red band indices RBD and KBBI which appear to be effective for assisting *K. brevis* bloom detection and classification respectively. These techniques take advantage of the low backscattering characteristics of *K. brevis* which allows RBD values to increase with increasing chlorophyll concentrations due to chlorophyll fluorescence, while at the same time, KBBI values also increase with

increasing chlorophyll concentration for *K. brevis* blooms but remains relatively small for non-*K. brevis* blooms.

The thresholds for bloom detection and *K. brevis* bloom classification were derived using simulated data coupled with the satellite data of known bloom events. Both techniques were successfully applied to MODIS data to detect, monitor and classify *K. brevis* blooms in the Gulf of Mexico to be efficient if used together. Different *K. brevis* bloom events documented in the literature were successfully detected and in addition, the *K. brevis* bloom event that took place in late 2004 on the WFS was traced for several weeks using the proposed bloom detection technique.

Our results provide a way for assisting the detection of toxic dinoflagellate *K. brevis* blooms and differentiating them from other blooms or bloom like features such as CDOM-rich plumes using satellite ocean color measurements. In particular, we show that these indicators improve on traditional algorithms such as FLH to correctly identify the potential bloomed areas and to distinguish *K. brevis* blooms from other blooms, plumes, and even shallow bottom reflectance. While the general thresholds developed provide a reasonably robust set of indicators, more extensive observations are needed to fine tune these and explore potential difficulties.

References

1. http://www.floridaconservation.org/

2. J. H. Landsberg, and K. A. Steidinger, "A historical review of *Gymnodium breve* red tides implicated in mass mortalities of the manatee (*Trichechus manatus latiriostris*) in Florida, USA," In: Reguera, B., Blanco, J., Fernandez, M.L., Wyatt, T. (Eds.), Proceedings of the 8th International Conference on Harmful Algal Blooms, Vigo, Spain, pp. 97-100, (1998)

3. W. H. Hemmert, "The public health implications of *Gymnodinium breve* red tides, A review of the literature and recent events" In: LoCicero, V.R. (Eds.), Proceedings of the First International Conference on Toxic Dinoflagellate Blooms, pp. 489-497, (1975)

4. S. Asai, J. J. Krzanowski, W. H. Anderson, D. F. Martin, J. B. Polson, R. F. Lockey, S. C. Bukantz, and A. Szentivanyi, "Effects of the toxin of red tide, *Ptychodiscus brevis*, on cannie tracheal smooth muscle: a possible new asthma-triggering mechanism," J. Allerg. Clinic. Immunol. 69, 418-428, (1982)

5. J. P. Cannizzaro, K. L. Carder, F. R. Chen, C. A. Heil, and G. A. Vargo, "A novel technique for detection of the toxic dinoflagellate *Karenia brevis* in the Gulf of Mexico from remotely sensed ocean color data," Continent. Shel. Res. 28, 137-158, (2008)

6. K. L. Mahoney, "Backscattering of light by *Karenia brevis* and implications for optical detection and monitoring," PhD dissertation, Univ. of South. Miss., Stennis Space Cent. (2003)

7. K. L. Carder, R. G. Steward, "A remote-sensing reflectance model of a red-tide dinoflagellate off west Florida," Limnol. Oceanogr. 30, 286-298, (1985)

8. O. Schofield, J. Kerfoot, K. Mahoney, M. Moline, M. Oliver, S. Lohrenz, and G. Kirkpatrick, "Vertical migration of the toxic dinoflagellate *Karenia brevis* and the impact on ocean optical properties," J. Geophys. Res., 111, (2006)

9. G. J. Kirkpatrick, D. F. Millie, M. A. Moline, O. Schofield, "Optical discrimination of a phytoplankton species in natural mixed populations," Limnol. Oceanogr. 45, 467-4718, (2000)

10. D. F. Millie, G. J. Kirkpatrick, B. T. Vinyard, "Relating photosynthetic pigments and in vivo optical density spectra to irradiance for the Florida red-tide dinoflagellate *Gymnodinium breve*," Marine Ecology Progress Series 120, 65-75, (1995)

11. D. F. Millie, O. M. Schofield, G. J. Kirkpatrick, G. Johnsen, P. A. Tester, B. T. Vinyard, "Detection of harmful algal blooms using photopigments and absorption signatures: a case study of the Florida red tide dinoflagellate, *Gymnodinium breve*," Limnol. Oceanogr. 42, 1240-1251, (1997)

12. S. E. Lohrenz, G. L. Fahnenstiel, G. J. Kirkpatrick, C. L. Carroll, K. A. Kelly, "Microphotometric assessment of spectral absorption and its potential application for characterization of harmful algal species," Journal of Phycology 35, 1438-1446, (1999)

13. A. Morel, and Y. Ahn, "Optics of heterotrophic nanoflagellates and ciliates: A tentative assessment of their scattering role in oceanic waters compared to those of bacteria and algal cells," J. Mar: Res. 49, 177-202, (1991)

14. D. Stramski, and D. A. Kiefer, "Light scattering in microorganisms in the open ocean," Prog. Oceanogr. 28, 343-383, (1991)

15. O. Ulloa, S. Sathyendranath, and T. Platt, "Effect of the particle-size distribution on the backscattering ratio in seawater," Appl. Opt. 33, 7070-7077, (1994)

16. M. S. Twardowski, E. Boss, J. B. Macdonald, W. S. Pegau, A. H. Barnard, and J. R. V. Zaneveld, "A model for estimating bulk refractive index from the optical backscattering ratio and the implications for understanding particle composition in case I and case II waters," J. Geophys. Res. 106, 14129-14142, (2001)

17. R. P. Stumpf, M. E. Culver, P. A. Tester, M. Tomlinson, G. J. Kirkpatrick, B. A. Pederson, E. Truby, V. Ransibrahmanakul, and M. Soracco, "Monitoring *Karenia brevis* blooms in the Gulf of Mexico using satellite ocean color imagery and other data," Harmful Algae 2, 147-160, (2003)

18. J. E. O'Reilly, S. Maritorena, D. Siegel, M. C. O'Brien, D. Toole, B. G., Mitchell, et al., "Ocean color chlorophyll a algorithms for SeaWiFS, OC2, and OC4: version 4," In: Hooker, S. B. & Firestone, E. R. (Eds.), *SeaWiFS Postlaunch Calibration and Validation Analyses, Part 3 SeaWiFS Postlaunch Technical Report Series*, (pp. 9-23) Greenbelt, Maryland: NASA, Goddard Space Flight Center (2000)

19. H. R. Gordon, D. K. Clark, J. W. Brown, O. B. Brown, R. H. Evans, W. W. Broenkow, "Phytoplankton pigment concentrations in the Middle Atlantic Bight: comparison of ship determinations and CZCS estimates," Appl. Opt. 22, 20-36, (1983)

20. K. L. Carder, F. R. Chen, Z. P. Lee, S. K. Hawes, D. Kamykowski, "Semi-analytic moderate-resolution imaging spectrometer algorithms for chlorophyll a and

absorption with bio-optical domains based on nitrate-depletion temperatures," J. Geophy. Res. 104, 5403-5422, (1999)

21. C. Hu, F. E. Muller-Karger, C. Taylor, K. L. Carder, C. Kelble, E. Johns, and C. A. Heil, "Red tide detection and tracing using MODIS fluorescence data: A regional example in SW Florida coastal waters," Remote Sens. Environ. 97, 311-321, (2005)

22. A. Gilerson, J. Zhou, S. Hlaing, I. Ioannou, R. Amin, B. Gross, F. Moshary, and S. Ahmed, "Fluorescence contribution to reflelctance spectra for a variety of coastal waters," Proc. Of SPIE 6680 (2007)

23. A. Gilerson, J. Zhou, S. Hlaing, I. Ioannou, J. Schalles, B. Gross, F. Moshary, and S. Ahemd, "Fluorescence component in the reflectance spectra from coastal waters. Dependence on water composition," Opt. Express, 15, 15702-15721 (2007)

24. A. Gilerson, J. Zhou, S. Hlaing, I. Ioannou, B. Gross, F. Moshary, and S. Ahmed, "Fluorescence component in the reflectance spectra from coastal waters. II. Performance of retrieval algorithms," Opt. Express 16, 2446-2460, (2008)

25. R. Amin, J. Zhou, A. Gilerson, B. Gross, F. Moshary, and S. Ahmed, " Detection of *Karenia brevis* harmful algal blooms in the West Florida Shelf using red bands of MERIS Imagery," OCEANS 08 MTS/IEEE Quebec, Canada, 15-18 Sept. (2008)

26. http://oceancolor.gsfc.nasa.gov

27. H. R. Gordon, and M. Wang, "Retrieval of water-leaving radiance and aerosol optical thickness over the oceans with SeaWiFS: a preliminary algorithm," Appl. Opt. 33, 443-452 (1994)

28. M. Wang, and W. Shi, "Estimation of ocean contribution at MODIS near infrared wavelengths along the east coast of the U.S.: two case studies," Geophys. Res. Lett. 32, L13606, doi: 10.1029/2005GL022917,(2005)

29. Z. P. Lee, K. L. Carder, C. D. Mobley, R. G. Steward, and J. S. Patch, "Hyperspectral remote sensing for shallow waters: I. A semi-analytical model," Appl. Opt. 37, 6329-6338, (1998)

30. Z. P. Lee, K. L. Carder, C. D. Mobley, R. G. Steward, and J. S. Patch, "Hyperspectral remote sensing for shallow waters: 2. Deriving bottom depths and water properties by optimization" Appl. Opt. 38, 3831-3843, (1999)

31. R. Pope, and E. Fry, "Absorption spectrum (380 – 700 nm) of pure waters: II. Integrating cavity measurements" Appl. Opt. 36, 8710-8723, (1997)

32. Z. P. Lee, http://www.ioccg.org/groups/OCAG_data.html

33. A. Morel, "Optical properties of pure water and pure seawater," in *Optical Aspects of Oceanography,* N. G. Jerlov and E. S. Nielsen, eds., (Academic, New York, 1974)

34. Z. P. Lee, and K. L. Carder, "Band-ratio of spectral-curvature algorithms for satellite remote sensing?" Appl. Opt. 39, 4377-4380, (2000)

35. T. J. Smayda, "Harmful algal blooms: their ecophysology and general relevance to phytoplankton blooms in the sea," Limnol. Oceanogr. 42, 1137-1153, (1997)

36. D. Stramski, A. Bricaud, and A. Morel, "Modeling the Inherent Optical Properties of the Ocean Based on the Detailed Composition of the Planktonic Community," Appl. Opt. 40, 2929-2945 (2001)

37. C. S. Roesler, and E. Boss, "Spectral beam attenuation coefficient in the ocean color inversion" Geophys. Res. Lett. 30, 1468, doi:10.1029/2002GL016185 (2003)

38. Y. Huot, C. A. Brown, and J. J. Cullen, "New algorithms for MODIS sun-induced chlorophyll fluorescence and a comparison with present data products" Limnol. Oceanogr. Methods 3, 108-130, (2005)

39. J. Zhou, A. Gilerson, I. Ioannou, S. Hlaing, J. Schalles, B. Gross, F. Moshary, and S. Ahmed, "Retrieving quantum yield of sun-induced chlorophyll fluorescence near surface from hyperspectral in-situ measurement in productive water," Opt. Express 16, 17468-17483 (2008)

40. W. W. Gregg, and K. L. Carder, "A simple spectral solar irradiance model for cloudless maritime atmospheres," Limnol. Oceanogr. 35, 1657-1675, (1990)

41. A. Albert, and C. D. Mobely, "An analytical model for subsurface irradiance and remote sensing reflectance in deep and shallow case-2 waters," Opt. Express 11, 2873-2890, (2003)

42. A. Morel, and S. Maritorena, "Bio-optical properties of ocean waters: A reappraisal" J. Geophys.l Res. 106, 7163-7180, (2001)

43. http://oceancolor.gsfc.nasa.gov/DOCS/MSL12/master_prodlist.html/#nLw

44. J. J. Walsh, J. K. Jolliff, B. P. Darrow, J. M. Lenes, S. P. Milroy, A. Remsen, D. A. Dieterle, K. L. Carder etc., "Red tides in the Gulf of Mexico: where, when, and why?" J. Geophy. Res. 111, C11003, (2006)

45. K. L. Carder, J. P. Cannizzaro, F. R. Chen, C. Hu, " Detecting HAB's in the Gulf of Mexico: Problems with atmospheric correction and shallow waters," MODIS Science Team Meeting, (2005)

46. FWRI, http://www.floridamarine.org

47. R. Amin, A. Gilerson, J. Zhou, B. Gross, F. Moshary, and S. Ahmed, " Impacts of atmospheric corrections on algal bloom detection techniques," 89th AMS Annual Meeting, Phoenix, Arizona, 11-15 Jan, (2009)

48. M. C. Tomlinson, R. P. Stumpf, V. Ransibrahmanakul, E. W. Truby, G. J. Kirkpatrick, B. A. Pederson, G. A. Vargo, C. A. Heil, "Evaluation of the use of SeaWiFS imagery for detecting *Karenia brevis* harmful algal blooms in the eastern Gulf of Mexico," Remote Sens. Environ. 91, 293-303, (2004)

49. http://www.nasa.gov/centers/goddard/news/topstory/2004/0826planktonglow.html

50. http://nasascience.nasa.gov/earth-science/applied-sciences/national-applications/coastal-managment

51. http://coastwatch.noaa.gov/hab/bulletins_ns.htm

52. C. Hu, F. E. Muller-Karger, and P. W. Swarzenski, "Hurricanes, submarine groundwater discharge, and Florida's red tides," Geophys. Res. Lett. 33, L11601, doi: 10.1029/2005GL025449, (2006)

53. http://www.tpwd.state.tx.us/landwater/water/environconcerns/hab/redtide/status.phtml

54. A. Subramaniam, E. J. Carpenter, and P. G. Falkowski, "Bio-optical properties of the marine diazotrophic cyanobacteria *Trichodesmium spp*. II. A reflectance model for remote sensing," Limnol. Oceanogr. 44, 618-627, (1999)

55. D. MacKee, A. Cunningham, D. Wright, and L. Hay, "Potential impacts of nonalgal materials on water-leaving Sun induced chlorophyll fluorescence signals in coastal waters," Appl. Opt. 46, 7720-7729, (2007)

56. M. C. Tomlinson, T. T. Wynne, and R. P. Stumpf, "An evaluation of remote sensing techniques for enhanced detection of the toxic dinoflagellate, *Karenia brevis*," Remote Sens. Environ., doi:10.1016/j.rse.2008.11.003, (2008)

57. C. Hu, Z. P. Lee, F. E. Muller-Karger, and K. L. Carder, "Application of an optimization algorithm to satellite ocean color imagery: A case study in Southwest

Florida coastal waters," In J. Frouin, Y. Yuan, & H. Kawamura (Eds.) SPIE Proceedings. *Ocean Remote Sensing and Applications*, vol. 4892 (pp. 70-79). Bellingham, WA: SPIE, (2003)

CHAPTER 3 IMPACTS OF ATMOSPHERIC CORRECTIONS ON ALGAL BLOOM DETECTION TECHNIQUES

3.1 Introduction

Bio-optical retrieval algorithms based on blue-green reflectance ratios suffer severely in the coastal waters due to imperfect atmospheric corrections and spectral interferences from organic and inorganic components in the water, which furthermore, don't necessarily correlate with chlorophyll in the coastal waters. Standard near-infrared (NIR) atmospheric correction algorithms often fails in the coastal waters because of higher turbidities which result in increased elastic reflectance and significant radiance contributions in NIR bands. Recently, an atmospheric correction algorithm using the short-wave infrared (SWIR) bands has been applied to turbid coastal waters. In this study we examine the performance of our recently proposed bloom detection technique called Red Band Difference (RBD) and toxic dinoflagellate *Karenia brevis* (*K. brevis*) bloom classification technique called *K. brevis* Bloom Index (KBBI) for use with Moderate Resolution Imaging Spectroradiometer (MODIS) data, corrected for the atmosphere, using NIR and SWIR atmospheric correction algorithms. Our analysis shows that both atmospheric correction algorithms are unsatisfactory, giving negative normalized water-leaving signals at the 412nm band for the bloomed area, which is an indication of a failure of atmospheric correction. Standard reflectance band ratio algorithms applied to this inappropriately atmospherically corrected signal give different and inaccurate results with either atmospheric correction algorithm. However, the RBD

values retrieved from either atmospherically corrected data give nearly the same results ($r^2 = 0.99$) for the bloomed region while the KBBI values retrieved from either atmospherically corrected data seems to be less correlated ($r^2 = 0.64$).

3.2 Background

The fundamental measurement in ocean color remote sensing is the water-leaving radiance or the upwelling spectral distribution of the radiance from the ocean. Geophysical parameters such as chlorophyll concentrations can be retrieved from this water-leaving signal since it contains information about the water columns. Only about 10% of the total signal measured by the ocean color sensors contains information about the waters and the rest represents scattering from aerosols and air molecules. The goal of the atmospheric corrections over the ocean is to remove contributions from atmosphere and reflection from the sea surface.

Gordon and Wang (1994) [1] developed an atmospheric correction scheme for the Open Ocean where the aerosol contribution was estimated using Top of the Atmosphere (TOA) radiance/reflectance signals obtained from near infrared (NIR) bands (for MODIS 748-869nm). This approach assumes that ocean is optically black in the NIR bands due to the strong water absorption in this region of the spectrum. Although this technique works well in the Open Ocean, it breaks down in optically complex coastal waters, since black pixel approximation no longer holds true due to strong reflections from organic and inorganic particulate matters. If water-leaving radiance is not negligible in the NIR bands

then the retrieved aerosol loading will be overestimated, resulting in underestimated water-leaving radiances.

To avoid this problem, another atmospheric correction approach for coastal water was proposed [2] which uses short wave infrared (SWIR) bands (i.e., MODIS 1240nm and 2130nm). This approach is based on the fact that ocean water absorbs strongly in this spectral region, and the contributions of the in-water constituents are negligible and can safely be considered dark. However, at these long wavelengths the atmospheric reflectance itself is significantly weaker and spectral features, due to absorbing aerosols or fine urban modes, are particularly difficult to resolve.

Retrieved ocean products in the coastal waters are often inaccurate due to inappropriate atmospheric correction on top of many other contaminations such as CDOM and inorganic particulate matters. Although atmospheric correction algorithms are improving, it still remains a challenge to correct for the atmosphere particularly over the turbid waters. So, it is important to develop techniques that are less sensitive to the atmospheric correction algorithms. The main objective of this study is to analyze impacts of atmospheric correction algorithms on our recently proposed bloom detection technique called Red Band Difference (RBD) and *Karenia brevis* (*K. brevis*) bloom classification technique called *K. brevis* Bloom Index (KBBI).

3.3 Atmospheric corrections

The signal received at the TOA by an ocean color satellite sensor can be expressed according to [3] as

$$L_t(\lambda) = L_r(\lambda) + L_A(\lambda) + t_u(\lambda)L_{wc}(\lambda) + T_u(\lambda)L_g(\lambda) + t_u(\lambda)L_w(\lambda) \quad (1)$$

where $L_r(\lambda)$, $L_A(\lambda)$, $L_{wc}(\lambda)$, $L_g(\lambda)$, and $L_w(\lambda)$ are the contributions due to molecular scattering (Rayleigh), aerosol and Rayleigh-aerosol scattering, whitecaps, sun glint, and ocean water, respectively. Here $T_u(\lambda)$ and $t_u(\lambda)$ are the direct and diffuse upwelling transmittances of the atmosphere. The radiance, L, can be converted to reflectance, ρ, using the relation $\rho = \pi L / (F_0 \cos\theta_0)$, where F_0 is the extraterrestrial solar irradiance, and θ_0 is the solar zenith angle.

The reflectance contributed by whitecaps is estimated from the surface wind and subtracted from measured reflectance/radiance. The surface atmospheric pressure and wind speed are used to compute the Rayleigh scattering which is then subtracted from the whitecap corrected reflectance/radiance. The algorithm then selects from a family of aerosol models using signals from NIR or SWIR bands and estimates the aerosol contribution in each of the visible wavelength bands. After subtraction of the aerosol contribution, the water-leaving reflectance/radiance is obtained in each of the visible bands by dividing by the diffuse atmospheric transmittance.

3.4 Results

In coastal waters, the standard NIR atmospheric correction [1] often fails due to higher turbidity and consequently significant higher radiance contributions in the NIR bands. Since the water-leaving radiance at NIR can no longer be considered negligible

for the use of atmospheric correction for extreme blooms [3, 4], negative readings may result in the blue-green bands due to the over-correction of the atmosphere [5]. More recently an atmospheric correction scheme using the short-wave infrared (SWIR) bands has been proposed [2] for turbid coastal waters, and has become part of the operational SeaDAS environment. Clearly, the less a bloom retrieval index is sensitive to atmospheric correction uncertainties the better, so we next examine performance of our RBD and KBBI techniques for different atmospheric correction algorithms.

Fig. 1a shows two normalized water leaving radiance spectra averaged over 3 by 3 pixels taken from the same MODIS (Aqua) image of 13 Nov 2004 [6] from the area around (25.73ºN and 82.11ºW) but atmospherically corrected using standard NIR and SWIR algorithms. The negative signal at 412nm band, shown with an "orange, circle" in Fig. 1a, is an indication of the atmospheric correction failure, meaning that the signal is overcorrected for the atmosphere which is often the case in bloomed and coastal waters. Although SWIR seems to do a little bit better than NIR in the bloomed region (Fig 1a), they both give a negative signal at the blue band edges, an indication of the limitations of both algorithms, with errors in the atmospheric correction schemes clearly larger for shorter wavelengths. Thus, retrievals using blue-green band ratio algorithms with the imperfect atmospheric corrections will result in different and inaccurate results for different atmospheric correction algorithms.

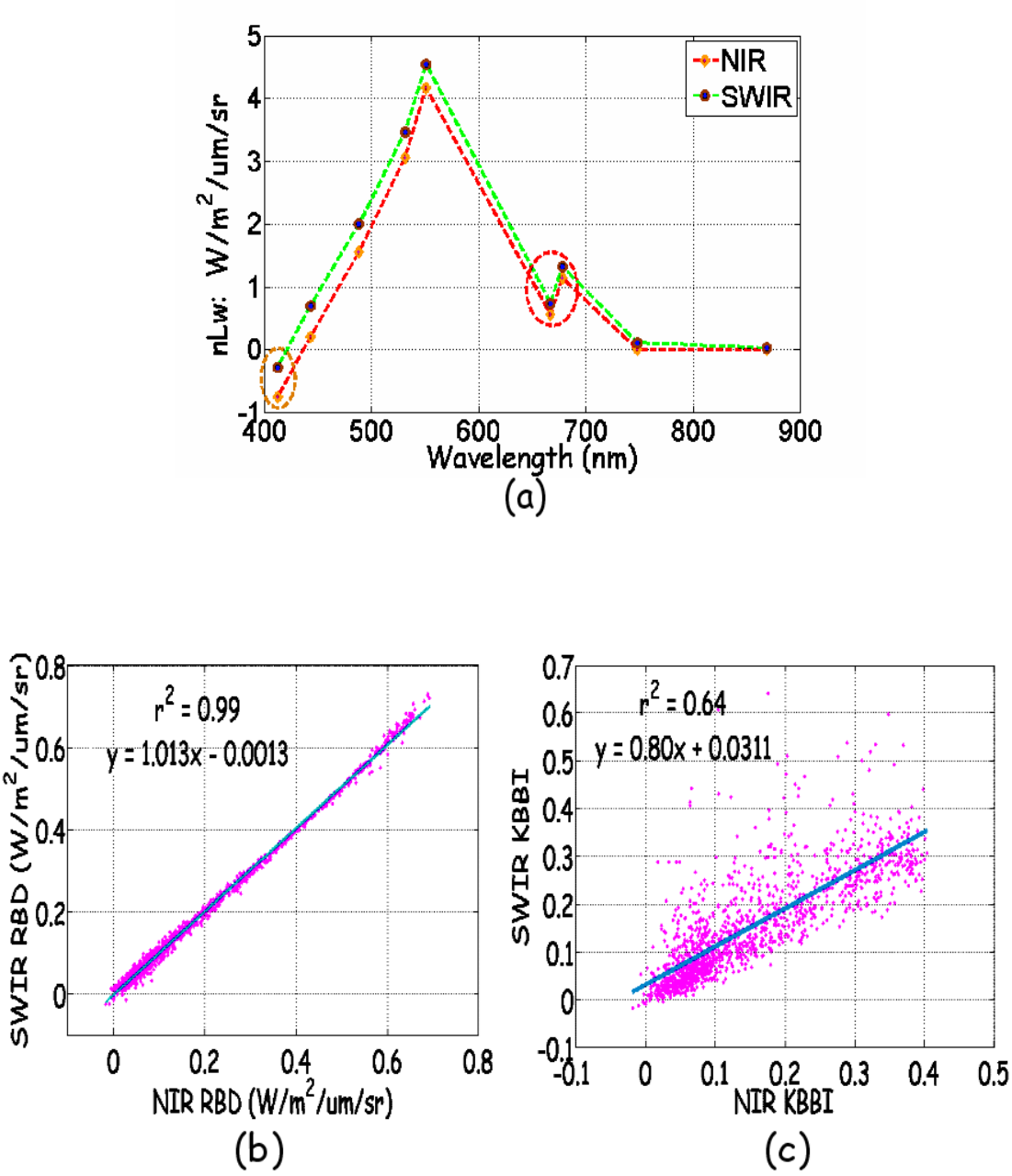

Fig. 1. (a) Normalized-water leaving radiance spectra of *K. brevis* bloom taken from the MODIS (Aqua) image of 13 Nov 2004 (25.73ºN and 82.11ºW) using different atmospheric correction: NIR and SWIR algorithms. The orange circled area indicates the atmospheric correction failure and the red circled area indicates the fluorescence peak. (b) RBD value with SWIR vs. RBD with NIR (c) KBBI value with SWIR vs. KBBI with NIR. The data are from the same image in (a) containing the region between (25.9ºN - 25.5ºN) and (81.9ºW - 82.3ºW).

Fig. 1b demonstrates the relative insensitivity of the RBD technique, which is focused on a small spectral range near the red chlorophyll fluorescence spectrum, on NIR and SWIR atmospheric correction algorithms. The data for Fig. 1b is taken from MODIS Aqua sensor image containing data from the regions between (25.9ºN - 25.5ºN) and (81.9ºW - 82.3ºW) on 13 Nov 2004. This region includes *K. brevis* bloomed areas as well as neighboring pixels which may contain *K. brevis* cells but in low concentrations. Our analysis shows that the RBD values are nearly the same with either atmospheric correction algorithm (Fig. 1b) for the selected regions. This is not surprising, since with RBD we are calculating the difference between the two bands which doesn't change if the spectrum is shifted up or down by different atmospheric correction algorithms, as oppose to spectral band ratios which change significantly even with a small shift in the absolute magnitudes of the bands.

3.5 Discussion

Our analysis shows that both atmospheric correction algorithms are unsatisfactory over the bloomed region, giving negative normalized water-leaving signals at blue-green bands. These negative $nLw(\lambda)$ values are primarily due to the fact that waters containing large accumulations of *K. brevis* species have a relatively strong water-leaving radiance in the near-infrared bands, while at the same time are absorbing strongly in the blue-green region, which leads to possible errors in the atmospheric correction and underestimation of $nLw(\lambda)$ in the blue and green bands of MODIS. Reflectance band ratio algorithms applied to this inappropriately atmospherically corrected signal gives

different and inaccurate results with either atmospheric correction algorithm. Results for the RBD bloom detection technique are found to be similar with either atmospheric correction algorithm. This is due to the fact that for this technique we are using the difference in magnitude of the water-leaving radiance signal at two adjacent red bands, and since these two bands are relatively close spectrally, 667nm and 678nm, the magnitude of the optical impact of the atmosphere will be very nearly the same on either band, and also when we calculate the difference of the two bands it remains nearly the same regardless of the shift the whole spectrum. This is in marked contrast to the impact of the atmosphere on the ratio of signal magnitudes at these bands. In our previous studies [7, 8], simulations for *K. brevis*, which is known to be characterized by weak backscatter, both because its own backscatter is low due to its low index of refraction, and also due to the typically low cohort submicron particulate concentrations typically associated with it, show that the *K. brevis* chlorophyll concentration strongly correlates with the RBD values for high chlorophyll ($>1 mg/m^3$). It should be possible to evolve empirically based relationships between RBD and *K. brevis* chlorophyll concentrations using in situ data. The nearly insensitivity of the RBD technique to atmospheric corrections in addition to the less sensitivity to CDOM [6, 7] may enable us to retrieve chlorophyll more accurately than the blue-green reflectance ratio algorithms for low backscattering blooms such as *K. brevis* that blooms regularly in the Gulf of Mexico particularly in the West Florida Shelf.

The KBBI technique is somewhat sensitive to the atmospheric corrections. However, it is still possible using either atmospheric correction scheme to identify *K. brevis* bloomed areas. While in general, the KBBI technique could identify potential *K.*

brevis bloomed area using data corrected with either atmospheric correction, the SWIR algorithm does more poorly in the offshore pixels and often gives noise values of KBBI (positive and negative false bloom alarm in nearby pixels). This is because the MODIS SWIR bands are designed for the land and have substantially lower signal-to-noise ratio (SNR) values. So the signals received in the SWIR bands in offshore pixels are low, and often within the noise level. Thus the overall performance of NIR algorithm is found to be better for use with KBBI than the SWIR algorithm, with the exception that NIR gives more false positive bloom alarms at the cloud edge pixels and spurious results for the stripe regions at the ends scan lines. Probably a combined NIR-SWIR atmospheric correction approach would be the best approach for the KBBI technique although it still needs to be verified.

3.6 Atmospheric Corrections Assessment

Our results show that both NIR and SWIR atmospheric correction approach fail in the bloomed regions which can lead to poor retrieval results particularly when band ratio algorithms are used to retrieve geophysical parameters such as chlorophyll which is often used to quantify blooms. We have shown that our bloom detection technique performs equally well with MODIS standard NIR and SWIR algorithms unlike the traditional band ratio algorithms such as standard chlorophyll retrievals. Our classification technique also performs reasonably well with the either atmospheric correction scheme for the bloomed regions.

References

1. H. R. Gordon, and M. Wang, "Retrieval of water-leaving radiance and aerosol optical thickness over the oceans with SeaWiFS: a preliminary algorithm," Appl. Opt. 33, 443-452 (1994)

2. M. Wang, and W. Shi, "Estimation of ocean contribution at MODIS near infrared wavelengths along the east coast of the U.S.: two case studies," Geophys. Res. Lett. 32, L13606, doi: 10.1029/2005GL022917, (2005)

3. R. Amin, A. Gilerson, J. Zhou, B. Gross, F. Moshary, and S. Ahmed, " Impacts of atmospheric corrections on algal bloom detection techniques," 89th AMS Annual Meeting, Phoenix, Arizona, 11-15 Jan, (2009)

4. D. A. Siegel, M. Wang, S. Maritorena, W. Robinson, "Atmospheric correction of satellite ocean color imagery: the black pixel assumption," Appl. Opt. 39, 3582-3591, (2000)

5. C. Hu, K. L. Carder, F. E. Muller-Karger, "Atmospheric correction of SeaWiFS imagery over turbid coastal waters: a practical method," Remote Sens. Environ. 74, 195-206, (2000)
6. C. Hu, F. E. Muller-Karger, C. Taylor, K. L. Carder, C. Kelble, E. Johns, and C. A. Heil, "Red tide detection and tracing using MODIS fluorescence data: A regional example in SW Florida coastal waters," Remote Sens. Environ. 97, 311-321, (2005)

7. R. Amin, J. Zhou, A. Gilerson, B. Gross, F. Moshary, and S. Ahmed, " Detection of *Karenia brevis* harmful algal blooms in the West Florida Shelf using red bands of MERIS Imagery," OCEANS 08 MTS/IEEE Quebec, Canada, 15-18 Sept. (2008)

8. R. Amin, J. Zhou, A. Gilerson, B. Gross, F. Moshary and S. Ahmed, "Use of MODIS Ocean Color Imagery for Improved Detection and Monitoring of *Karenia brevis* Blooms in the Gulf of Mexico," Ocean Optics XIX Tuscany, Italy, October 6-10, 2008

CHAPTER 4 MODIS AND MERIS DETECTION OF DINOFLAGELLATES BLOOMS USING THE RBD TECHNIQUE

4.1 Introduction

Harmful Algal Blooms (HABs) can lead to severe economical and ecological impacts particularly in the coastal areas and can threaten human and marine health. About three-quarter of these toxic blooms are caused by dinoflagellates species which are well known to migrate vertically. During the day, they migrate up to the surface for photosynthesis, and consequently, their dense aggregations produce strong bio-optical signals that are detectable by space borne optical satellite sensors. In this study we use our recently developed low backscattering bloom detection technique, the Red Band Difference (RBD), to detect various dinoflagellates blooms using both MODIS (Moderate Resolution Imaging Spectroradiometer) and MERIS (Medium Resolution Imaging Spectrometer) data and present the results which confirm the potentials of the RBD technique. Here we present examples of bloom detection in waters off Gulf of Mexico, Monterey Bay, South Africa, and East China Sea.

4.2 Background

Over past several decades, the frequency and severity of Harmful Algal Blooms (HABs), also known as red tides, has increased throughout the world. Eutrophication in estuaries and coastal waters has been considered a major factor causing HABs [1, 2]. Human and industrial activities have contributed to bring various pollutants required for

the increasing of HABs occurrence from land through river discharge. Even wet-deposition of atmospheric aerosols and other hazardous gases produced from fossil fuel burning can contribute to HABs. The HABs are becoming an increasingly frequent and hazardous disaster particularly in the coastal areas around the globe. In some part of the world, these toxic blooms have resulted in the collapse of ecosystem processes due to environmental stress while caused regional economic losses of 10 to 200 million dollars annually due to human health problems, commercial and recreational fishing closures, and cleanup coasts [3].

Dinoflagellates, the organisms that cause most red tides, are microscopic, single-celled organisms characterized by two whiplike structures, each called a flagellum which help them swim through the water. These species can produce some of the most powerful poisons in nature. When they bloom, they can discolor the water in red, but color may also be yellow, orange, brown, or reddish-brown. That's why scientists prefer the term HABs rather than red tides. Marine HABs are usually caused by dinoflagellates and take place in warm regions or seasons and in places which are richer in nutrients such as coastal waters influenced by agricultural activity from inland regions [4]. Freshwater HABs, due to dinoflagellates, are much less widespread than in the sea [5]. Approximately 50% of all red tide forming species and 75% of all HAB species are dinoflagellates [6, 7].

Dinoflagellates exhibit unique differences from diatoms for example in their adaptive ecologies which may be favoring their increasingly successful exploitation of coastal waters and global bloom expansion [8]. In general, it's believed that dinoflagellate blooms occurs in a basic red tide ecological zone of high irradiance, low

turbulence and elevated nutrients. Watermass stratification has been considered the essential physical condition that dinoflagellates require to bloom because of their relative inability, unlike diatoms, to tolerate the elevated shear-stress associated with water-column mixing, turbulence and high velocity, coastal currents [7, 9, 10]. Dinoflagellate motility provides a competitive advantage because their populations can migrate downward at night to acquire nutrients [11, 12]. When these populations migrate up to the surface for photosynthesis during the day, their dense aggregations produce strong bio-optical signals that are detectable by satellite and airborne optical sensors.

Backscattering of the light in the ocean is typically dominated by submicron particles [13, 14]. Since dinoflagellates usually require stratified water, mineral particles, which backscatter strongly due to their smaller size and higher index of refractions, may not exist in high concentrations in dinoflagellates bloomed waters. Furthermore, it also been suggested that zooplankton grazing pressure maybe lower on toxic dinoflagellates blooms due to their toxicity and larger size [15, 16]. So there may also not be much detritus matters in these types of blooms. As a result, the total backscattering signal in a dinoflagellates blooms maybe lower compare to blooms of other species such as diatoms [17] since algal particles exhibit weaker backscattering compare to non-algal particles [18]. When low backscattering blooming conditions exist, the red water leaving radiance signal becomes chlorophyll fluorescence dominated. Therefore, the Red Band Difference (RBD) technique can easily extract portion of this fluorescence signal to indicate bloom.

Detecting and monitoring of HABs are very important for protecting public health, wild and farmed fish and shellfish, and endangered species such as marine mammals. They can also affect the tourism industry and coastal business when dead fish

wash up on shore, when surf activity creates thick layers of smelly foam on beaches, or when local sea food is suspected to be inedible. As a result, methods need to be established to monitor and predict bloom formation and transport to mitigate their harmful effects on the surrounding ecosystems and local communities.

Detecting and monitoring HABs from field measurements is labor intensive and suffers from practical limitations on achievable temporal and spatial resolutions. Field measurements are typically made at discrete points and at discrete times, without much temporal continuity. To assist in the detection of blooms and the planning preparation of remedial measures to reduce health risks, etc., detection approaches with higher spatial and temporal resolutions are desirable. It is in this context that satellite Ocean Color sensors offer potential advantages for bloom detection and monitoring.

Many satellite HABs detection algorithms such chlorophyll anomaly [19] have been developed, but these don't work very well, particularly in optically complex turbid coastal waters due to the contamination from various organic and inorganic matters found in these waters, and therefore often don't correlate very well with chlorophyll. These problems are also increased by inaccurate atmospheric corrections. However, the RBD technique is nearly insensitive to atmospheric corrections, since it uses two very closely being bands where atmospheric impacts are nearly the same and also looks at band difference rather than ratios [20-22]. Furthermore, the RBD technique is less affected by CDOM, since CDOM absorption is very little in the red. Moreover, this technique uses water leaving radiance signal directly, rather than using some standard ocean color products such as chlorophyll, so no retrieval errors are associated with this technique.

Detecting blooms using remote sensing requires measurements of water leaving radiance in the red-NIR regions of the optical spectrum because bloom has a unique peak around this region [23]. However, the RBD technique requires measurements only in the red region of the optical spectrum. Therefore, this technique can be applied to the data from both MERIS (Medium Resolution Imaging Spectrometer) on ENVISAT satellite launched by the European Space Agency (ESA), and MODIS (Moderate Resolution Imaging Spectroradiometer) launched on both the Terra and Aqua satellites by the National Aeronautics and Space Administration (NASA). Both instruments cover wide swaths, providing near-daily images and have optical spectral bands in red-NIR region which can be used to detect various types of marine vegetations. By combining data from these sensors, cloud coverage problem, which is an issue for space borne optical sensors, can be reduced.

The objective of this study is to use our recently developed RBD bloom detection technique to detect various toxic dinoflagellates blooms since these species are the biggest concern for most of the coastal areas around the world. For this study we use data from both MODIS and MERIS sensors.

4.3 Data Processing and Methodology

4.3.1 Satellite data

The MERIS was launched in March 2002 and has provided systematic global coverage at 1200 m resolution since June of that year. Atmospherically corrected MERIS standard Level -2 reduced-resolution (RR) data was obtained from ESA website [24] for

various dinoflagellates blooms hot spots around the world. This Level-2 data contains normalized surface reflectance. Only reflectances at MERIS band 7 and 8 were used since the RBD is defined using these two channels. BEAM 4.5.1 Software was used to create and analyze the RBD images for the selected studied areas.

The MODIS imagery for the selected areas were obtained from the NASA Ocean Color Website [25] and processed to obtain the remote sensing reflectance ($R_{rs}(\lambda)$) for bands 13 and 14 using SeaDAS version 5.0.3. The top of the atmosphere signals were corrected for the atmosphere using the standard NIR atmospheric correction method [26] and the data was processed with a pixel size of 1km equal to the nominal pixel size of the sensor's ocean color bands. All the bloom images studied here were taken from the literature.

4.3.2 The RBD technique

As discussed above in Chapter 2, the RBD bloom detection technique was introduced in [20] and can be expressed as

$$RBD = nLw(\lambda_2) - nLw(\lambda_1) \tag{1}$$

Where the $nLw(\lambda)$ is the normalized water-leaving radiance which is defined as the upwelling radiance just above the sea surface, in the absence of an atmosphere, and with sun directly overhead. The λ_1 represents MODIS band 13 or MERIS band 7 and the λ_2 represents MODIS band 14 or MERIS band 8. The RBD technique was achieved based on the principle that dinoflagellates organisms such as *Karenia brevis* (*K. brevis*)

absorbs strongly around 675nm which causes $nLw(\lambda)$ to have a trough around this band. But because of the contribution of chlorophyll fluorescence emission centered on 685nm and relatively lower backscattering efficiency of these species, this trough is shifted toward shorter wavelengths around 667nm or below depending on the concentrations of chlorophyll and the quantum yield of chlorophyll fluorescence. Therefore, the signal around λ_2, which falls in the shoulder of the red-NIR water-leaving radiance peak, has higher values than the signal around λ_1 due to the chlorophyll fluorescence contribution. Simulation shows that the positive RBD values ($>1 mg/m^3$ of Chlorophyll) are primarily due to the fluorescence signal which correlates strongly with the chlorophyll concentration for low backscattering blooms such as *K. brevis*. So it may also be possible to quantify these blooms in terms of chlorophyll concentrations more accurately than the standard band ratio algorithms by developing some empirical relationship between the RBD values and the bloom chlorophyll concentrations using in situ data. Note that for this study we use MODIS and MERIS level-2 reflectance rather than the water leaving radiance to create RBD images.

4.4 Results of RBD Application to Different Locations

4.4.1 Gulf of Mexico

More than 40 species of toxic microalgae live in the Gulf of Mexico, but the most common is the toxic dinoflagellate *K. brevis* formerly named *Gymnodinium breve* [27]. Although *K. brevis* blooms have been reported throughout the Gulf of Mexico, they are most frequent along the West Florida Shelf (WFS) where they occur nearly every year,

usually between late fall and early spring but occasionally at other times of the year as well. *K. brevis* blooms have many negative impacts due to brevetoxin. This associated toxin causes death in fish, birds, and marine mammals [28]. It also can irritate human eyes and respiratory systems once it becomes airborne in sea spray [29, 30].

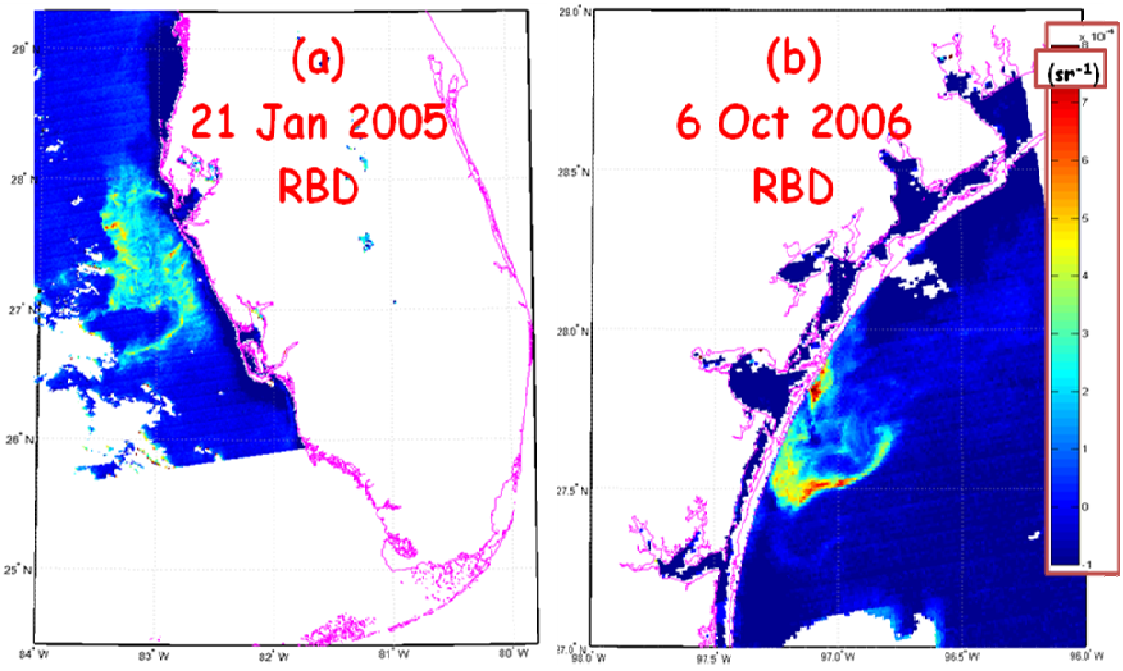

Fig. 1. Using MODIS data the RBD technique detects toxic dinoflagellate *K. brevis* blooms in (a) Florida on 21 January 2005 and (b) Texas on 6 October 2006.

Using the RBD bloom detection technique, we detected various toxic dinoflagellate *K. brevis* blooms in the Gulf of Mexico. Figure 1 demonstrates two examples of *K. brevis* bloom detection using MODIS data: one for Florida on 21 January 2005 [31] and the other for Texas on 6 October 2006 [32]. Furthermore, figure 2 demonstrates an example of *K. brevis* bloom tracing for several weeks using MERIS data for the 2004 bloom event. This bloom event took place between October and December

2004. According to [33] this bloom by mid-late November contained high concentrations ($>10^5 cells/l$) of *K. brevis* cells and caused higher mortalities of fish and dolphins. These results were found to match reasonably well with the cell count data from in situ measurements, obtained from [34].

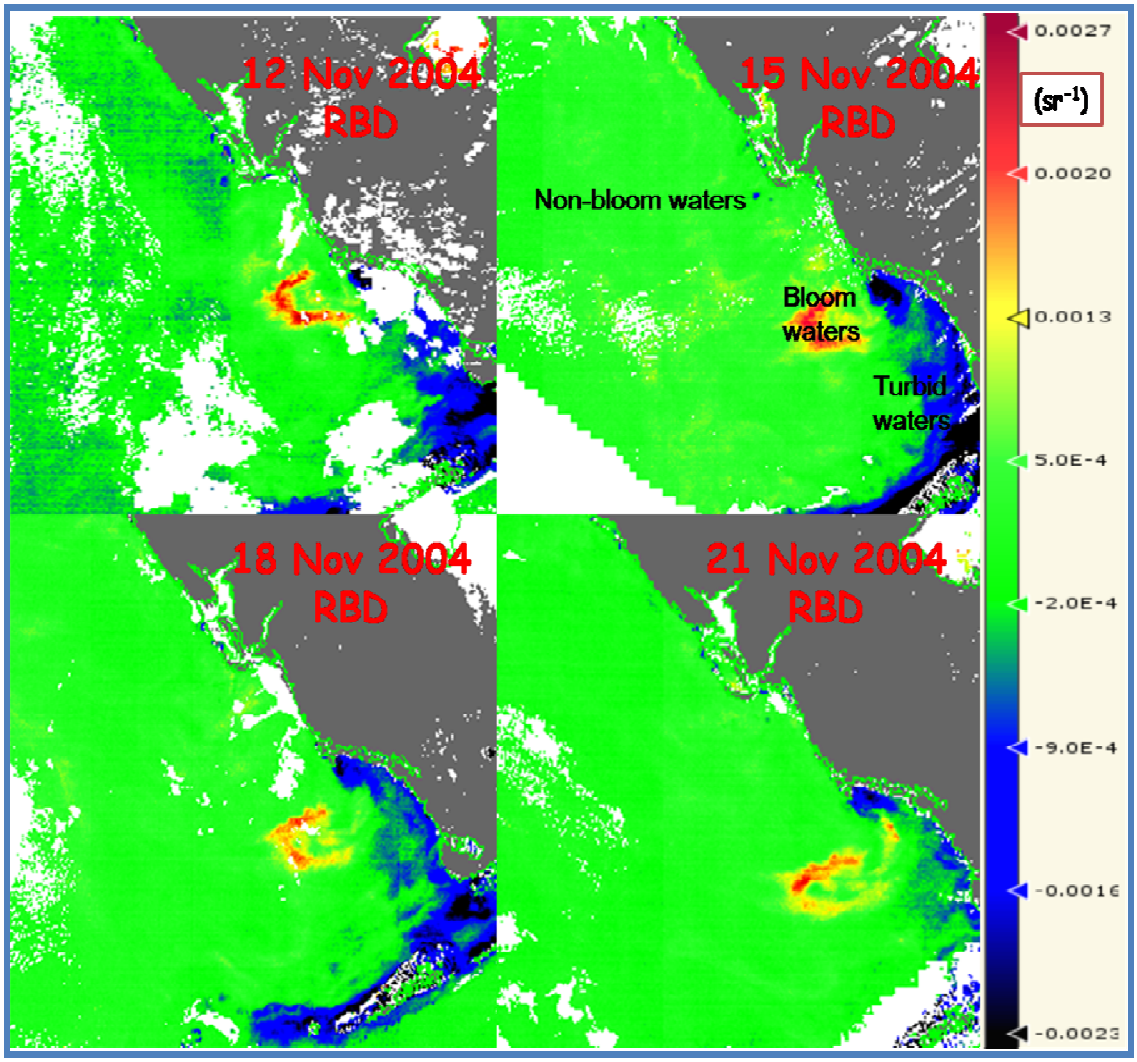

Fig. 2. MERIS RBD image series show the progression of a toxic dinoflagellate *K. brevis* bloom in the West Florida Shelf.

4.4.2 Monterey Bay

Monterey Bay frequently suffers from extreme dinoflagellates blooms, primarily between August and November and can persist for more than a month. These dinoflagellates blooms can contain surface chlorophyll concentrations exceeding 500 ug/l and often occupying ~5 to 80 km^2 [35]. According to [35], the maximum bloom frequency with high intensity occurs in a shallow (<25 m depth) area of the northeastern part of the bay when surface water is the warmest, low wind stress and retentive circulation which are favorable to dinoflagellates blooms. These blooms are usually caused by the dinoflagellates species such as Akashiwo, Cochlodinium and Ceratium [36, 37] which are known to exhibit strong vertical migratory behavior and aggregate near the surface for photosynthesis [38-40]. Because of their strong surface aggregations, they produce strong bio-optical signal which can be detected by space borne optical satellite sensors.

Figure 3 demonstrates example of dinoflagellates bloom detection in the Monterey Bay, California using both MODIS and MERIS data. Figure 3a shows the RBD image using MERIS data for November 3, 2007 while figure 3b shows the RBD image using MODIS data for 15 September 2006. The large bloom event of 2007 persisted from early October to mid-November and exceeded 500 ug/l of surface chlorophyll concentrations [35]. Although the spatial extant of these blooms are not as big as the *K. brevis* blooms in the Gulf of Mexico for example, often they are large enough to be detectable by optical satellite sensors even with the reduced-resolution imageries.

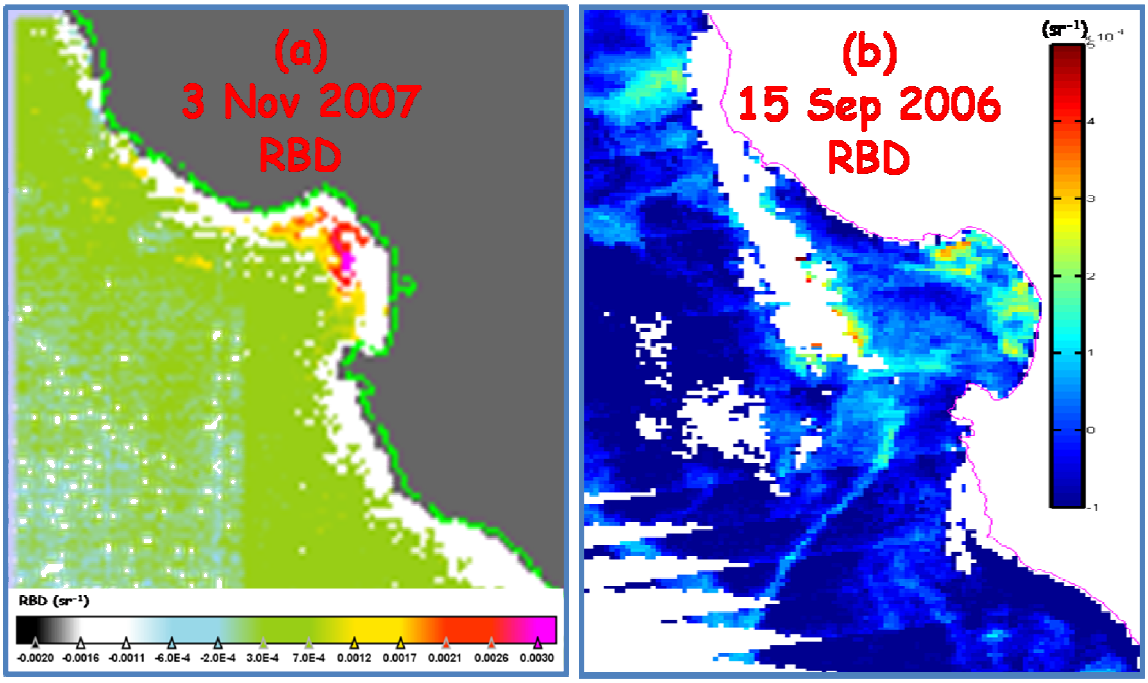

Fig. 3. (a) The MERIS reduce-resolution RBD image of extreme dinoflagellates bloom in the Monterey Bay, California on November 3 2007. (b) The MODIS RBD image detects dinoflagellates bloom in the Monterey Bay on 15 September 2006.

4.4.3 South Africa

The southern Benguela suffers from frequent occurrence of HABs most often composed of variety of dinoflagellate species [41]. These dinoflagellates blooms are usually caused by *Prorocntrum triestinum* and *Ceratium furca* [42] and often results in severe negative impacts to local marine ecosystems, communities and commercial marine industries. Collapse of these high biomass blooms can lead to hypoxic events and in extreme cases, the production of hydrogen sulphide, frequently causing extensive mortalities of marine organisms. Figure 4 demonstrates an example of dinoflagellates bloom detection using the RBD technique on the Western Coast of South Africa. This RBD bloom image was created using MERIS data for 25 April 2005[43].

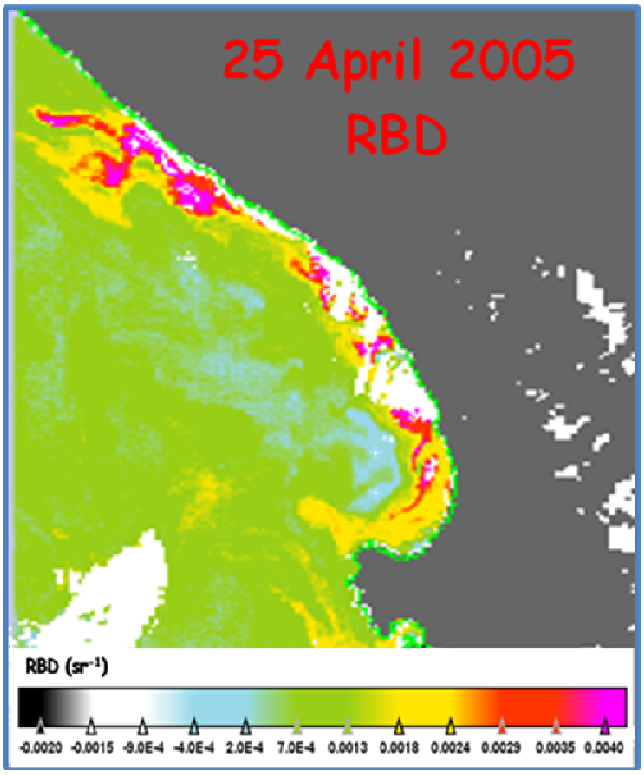

Fig. 4. The RBD image of MERIS reduced-resolution data for the Western Coast of South Africa on 25 April 2005. Clouds and invalid reflectances are masked to white. The area of high RBD values along the coast indicating the bloomed areas.

4.4.4 East China Sea

HABs occur most frequently in the East China Sea where Chinese biggest fish farm is located. These HABs have increased in the frequency and scale since 1998 often occupying 1000 km^2 and lasting for month [44]. These Chinese coastal areas are an important economic area because of rapid economic and population growth which has led to significant increases in wastewater and sewage discharge into the East China Sea. As a result, eutrophication and frequent HABs are very common in these waters usually from May to July [45]. Fisheries resources and mariculture operations are affected by these

events, which lead to a reduction in ecological diversity and health problems for the public.

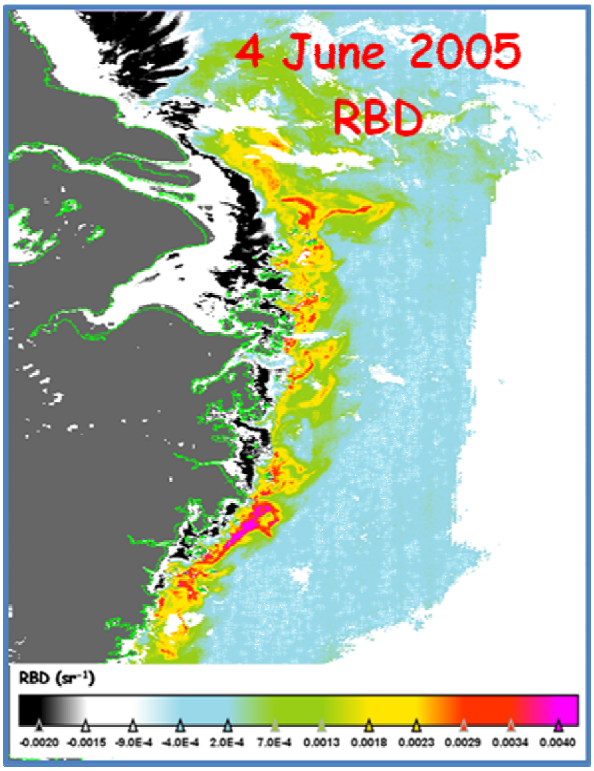

Fig. 5. MERIS reduce-resolution RBD image of water off the East China Sea on 4 June 2005. Cloud and invalid reflectances are masked in white while land is masked in gray.

Figure 5 demonstrates an example of dinoflagellates bloom detection in the East China Sea using the RBD technique. This RBD image was created using MERIS reduced-resolution data for 4 June 2005 [44]. According to the red tide bulletins of the State Oceanic Administration of China (SOA) and local government agencies, the red tides events with large scale occurred from 24 May to 13 June along Zhejian coastal regions in the East China Sea.

4.5 Discussion

Bloom detection using standard blue-green band ratio algorithms suffers severely in the coastal waters particularly from inaccurate atmospheric corrections and CDOM. Unfortunately, most of the toxic blooms occur in the coastal areas where nutrients are supplied through river discharge from land and also from the bottom through coastal upwelling. Detecting these coastal blooms and getting their precise locations are nearly impossible with blue green algorithms. However, red and red-NIR band difference algorithms such as RBD and Fluorescence Line Height (FLH) can be very useful to detect these blooms. This is because these techniques are nearly insensitivity to the atmospheric corrections and variability due to CDOM is lower since CDOM absorption is very little in the red-NIR region [20, 22, 46]. MODIS and MERIS sensors were designed with channels in the red and NIR region of the optical spectrum to detect chlorophyll fluorescence in the ocean surface. However, standard chlorophyll fluorescence retrieval using the FLH method suffers severely in the turbid coastal waters where high red peak values are primarily due to contributions from elastic scattering modulated by chlorophyll absorption rather than the fluorescence, thus falsely indicates blooms. In contrast, the RBD technique gives positive values in truly bloomed waters and negative values in highly scattering waters [20].

Because of the enhanced water stratification, possibly sediments are already settled to the bottom by the time bloom initiates. So, it should be reasonable to expect lower concentrations of sediments in the dinoflagellates bloomed waters. Furthermore, fewer detritus matters are also expected due to the lower zooplankton grazing pressure.

Thus, fewer non-algal particles maybe associated with the dinoflagellates blooms. As a result, the total backscattering signal maybe relatively lower compare to the blooms of other species such as diatoms since the backscattering signal should be dominated by the algal particles which are well known to backscatter weakly. When low backscattering blooms exist, the red spectral region becomes chlorophyll fluorescence dominant and the RBD can easily extract portion of this fluorescence signal to indicate blooms. However, it can be argued that water absorption is relatively high in the red, so the RBD technique would only detect blooms that are near the water surface. Fortunately, dinoflagellates are well known to aggregate towards the surface during the day for photosynthesis, which is when satellites can observe them, so water absorption would not be an issue.

RBD images computed using MERIS bands 7 and 8 or MODIS bands 13 and 14 can locate dinoflagellates blooms and this technique has many advantages over other blue-green and red-NIR techniques [20-22, 46]. However, the RBD images created using both MODIS and MERIS data showed significant noise near the cloud edge pixels due to the scattering from clouds which also affects nearby pixels. Furthermore, the RBD images created using MODIS data often showed striping at the end of each scan line due to the variations in detector response. However, both the striping and the noise at the cloud edge have significantly different appearances from the bloom patches and can be easily distinguished in observation.

4.6 Conclusion

Toxic dinoflagellates blooms are responsible for hundreds of millions of dollars in economic damages each year throughout the world. Our study proves that the RBD bloom detection technique is an effective tool for detection and monitoring of these toxic dinoflagellates blooms. Furthermore, this study also proves the importance of having red fluorescence channels on current and future ocean color satellites sensors. Detection with both MODIS and MERIS imagery are considered a success. However, further research is required possibly coupled with the in situ data to develop detection thresholds for each of these species.

References

1. A. J. McComb, (Ed.), "Eutrophic Shallow Estuaries and Lagoons," 240 pp., CRC Press, Boca Raton, Fla. (1995)

2. T. J. Smayda, "Novel and nuisance phytoplankton bloom in the sea: Evidence for global epidemic," in Toxic Marine Phytoplankton: Proceedings of the Fourth International Conference on Toxic Marine Phytoplankton, Held June 26 – 30 in Lund, Sweden, edited by E. Graneli et al., pp. 29–40, Elsevier Sci., New York, (1990)

3. P. Hoagland, and S. Scatasta, "The economic effects of harmful algal blooms," In E. Graneli and J. Turner, eds., Ecology of Harmful Algae. Ecology Studies Series. Dordrecht, The Netherlands: Springer-Verlag, Chap. 29, (2006)

4. C. V. Hoek, D. G. Mann and H. M. Jahns, "Algae. *An introduction to phycology*," Cambridge University Press: 627pp. (1995)

5. S. Rodriguez, A. Coute, L. Tenhage and G. Mascarell, "Peridiniopsis durandi sp. nova (Dinophyta), une nouvelle Dinophycee d'eau douce responsible de marees rouge," Algological Studies, 95: 15-29. (1999)

6. A. Sournia, "Red-tide and toxic marine phytoplankton of the world ocean: An inquiry into biodiversity," in *Harmful Marine Algal Blooms*, edited by P. Lassus et al., pp. 103-112, Lavoisier, Paris. (1995)

7. T. J. Smayda, "Harmful algal blooms: Their ecophysiology and general relevance to phytoplankton blooms in the sea," Limnol. Oceanogr., 42, 1137-1153, (1997)

8. T. J. Smayda, "Turbulence, watermass stratification and harmful algal blooms: An alternative view and frontal zones as pelagic seed banks," Harmful algae 1:95-112, (2002)

9. J. H. Ryther, "Ecology of autotrophic marine dinoflagellates with reference to red water condition," pp. 387-414 in The *Luminescence of Biological Systems*, F. H. Johnson, ed. American Association for the Advancement of Science, Washington, D.C. USA. (1955)

10. R. Margalef, M. Estrada, and D. Blasco, "Functional morphology of organisms involved in red tides, as adapted to decaying turbulence," pp. 89-94 in Toxic Dinoflagellate Blooms, Proceedings of the Second International Conference on toxic dinoflagellate blooms. D. L. Taylor and H. H. Seliger, eds. Elsevier, New York, NY. USA. (1979)

11. J. J. Cullen, and S. G. Horrigan, "Effects of nitrate on the diurnal vertical migration, carbon to nitrogen ratio, and the photosynthetic capacity of the dinoflagellate Gymnodinium splendens," *Mar. Biol. Berlin*, 62, 81-89. (1981)

12. S. I. Heaney, and R. W. Eppley, "Light, temperature and nitrogen as interacting factors affecting diel vertical migrations of dinoflagellates in culture," *J. Plankton Res., 3*(2), 331-344. (1981)

13. A. Morel, and Y. Ahn, "Optics of heterotrophic nanoflagellates and ciliates: A tentative assessment of their scattering role in oceanic waters compared to those of bacteria and algal cells," J. Mar: Res. 49, 177-202, (1991)

14. D. Stramski, and D. A. Kiefer, "Light scattering in microorganisms in the open ocean," Prog. Oceanogr. 28, 343-383, (1991)

15. E. J. Buskey, P. A. Montagna, A. F. Amos, and T. E. Whitledge, "Disruption of grazer populations as a contributing factor to the initiation of the Texas brown tide algal bloom", Limnol. Oceanogr., 42, 1215-1222 (1997)

16. O. Schofield, J. Kerfoot, K. Mahoney, M. Moline, M. Oliver, S. Lohrenz, and G. Kirkpatrick, "Vertical migration of the toxic dinoflagellate *Karenia brevis* and the impact on ocean optical properties," J. Geophys. Res., 111, (2006)

17. J. P. Cannizzaro, K. L. Carder, F. R. Chen, C. A. Heil, and G. A. Vargo, "A novel technique for detection of the toxic dinoflagellate *Karenia brevis* in the Gulf of Mexico from remotely sensed ocean color data," Continent. Shel. Res. 28, 137-158, (2008)

18. Z. P. Lee, http://www.ioccg.org/groups/OCAG_data.html

19. R. P. Stumpf, M. E. Culver, P. A. Tester, M. Tomlinson, G. J. Kirkpatrick, B. A. Pederson, E. Truby, V. Ransibrahmanakul, and M. Soracco, "Monitoring *Karenia brevis* blooms in the Gulf of Mexico using satellite ocean color imagery and other data," Harmful Algae 2, 147-160, (2003)

20. R. Amin, J. Zhou, A. Gilerson, B. Gross, F. Moshary and S. Ahmed, "Novel Optical Techniques for Detecting and Classifying Toxic Dinoflagellate *Karenia brevis* Blooms Using Satellite Imagery," Optics Express Vol. 17, Iss. 11, pp. 9126-9144 (2009)

21. R. Amin, A. Gilerson, J. Zhou, B. Gross, F. Moshary and S. Ahmed, "Impacts of Atmospheric Corrections on Algal Bloom Detection Techniques," 89th AMS Annual Meeting, Phoenix, Arizona, January 11-15, (2008)

22. R. Amin, J. Zhou, A. Gilerson, B. Gross, F. Moshary and S. Ahmed, "Use of MODIS Ocean Color Imagery for Improved Detection and Monitoring of *Karenia brevis*

Blooms in the Gulf of Mexico," Ocean Optics XIX Tuscany, Italy, October 6-10, (2008)

23. J. Gower, S. King, G. Borstad, and L. Brown, "Detection of intense plankton blooms using the 709nm band of the MERIS imaging spectrometer," *Int. J. Remote Sens*., 26, 2005-2012. (2005)

24. http://merci-srv.eo.esa.int/merci/welcome.do

25. http://oceancolor.gsfc.nasa.gov

26. H. R. Gordon, and M. Wang, "Retrieval of water-leaving radiance and aerosol optical thickness over the oceans with SeaWiFS: a preliminary algorithm," Appl. Opt. 33, 443-452 (1994)

27. http://www.floridaconservation.org/

28. J. H. Landsberg, and K. A. Steidinger, "A historical review of *Gymnodium breve* red tides implicated in mass mortalities of the manatee (*Trichechus manatus latiriostris*) in Florida, USA," In: Reguera, B., Blanco, J., Fernandez, M.L., Wyatt, T. (Eds.), Proceedings of the 8th International Conference on Harmful Algal Blooms, Vigo, Spain, pp. 97-100, (1998)

29. W. H. Hemmert, "The public health implications of *Gymnodinium breve* red tides, A review of the literature and recent events" In: LoCicero, V.R. (Eds.), Proceedings of the First International Conference on Toxic Dinoflagellate Blooms, pp. 489-497, (1975)

30. S. Asai, J. J. Krzanowski, W. H. Anderson, D. F. Martin, J. B. Polson, R. F. Lockey, S. C. Bukantz, and A. Szentivanyi, "Effects of the toxin of red tide, *Ptychodiscus brevis*, on cannie tracheal smooth muscle: a possible new asthma-triggering mechanism," J. Allerg. Clinic. Immunol. 69, 418-428, (1982)

31. K. L. Carder, J. P. Cannizzaro, F. R. Chen, C. Hu, " Detecting HAB's in the Gulf of Mexico: Problems with atmospheric correction and shallow waters," MODIS Science Team Meeting, (2005)

32. http://www.tpwd.state.tx.us/landwater/water/environconcerns/hab/redtide/status.phtml

33. C. Hu, F. E. Muller-Karger, C. Taylor, K. L. Carder, C. Kelble, E. Johns, and C. A. Heil, "Red tide detection and tracing using MODIS fluorescence data: A regional example in SW Florida coastal waters," Remote Sens. Environ. 97, 311-321, (2005)

34. FWRI, http://www.floridamarine.org

35. J. P. Ryan, J. F. R. Gower, S. A. King, W. P. Bissett, A. M. Fischer, R. M. Kudela, Z. Kolber, F. Mazzillo, E. V. Rienecker, and F. P. Chavez, "A coastal ocean extreme bloom incubator", Geophysical Research Lett, Vol 35, L12602, (2008)

36. J. P. Ryan, H. M. Dierssen, R. M. Kudela, C. A. Scholin, K. S. Johnson, J. M. Sullivan, A. M. Fischer, E. V. Rienecker, P. R. McEnaney, and F. P. Chavez, "Coastal ocean physics and red tides: An example from Monterey Bay, California," Oceanography 18, 246-255. (2005)

37. R. M. Kudela, J. P. Ryan, M. D. Blakely, J. Q. Lane and T. D. Peterson, "Linking the physiology and ecology of Cochlodinium to better understand harmful algal bloom events: A comparative approach," Harmful Algae, 7, 278-292 (2008)

38. D. Blasco, "Observations on the diel migration of marine dinoflagellates off the Baja California coast," Mar. Biol. Berlin, 46, 41-47. (1978)

39. J. G. Park, M. K. Jeong, J. A. Lee, K. J. Cho, and O. S. Kwon, "Diurnal vertical migration of a harmful dinoflagellate, Cochlodinium polykrikoides (Dinophyceae), during a red tide in coastal waters of Namhae Island, Korea," Phycologia, 40, 292-297. (2001)

40. P. L. Donaghay, J. M. Sullivan, J. E. Rines, J. Graff, A. K. Hanson, and D. V. Holliday, "The importance of swimming behavior in controlling the formation, maintenance and dissipation of thin optical layers," Eos Trans. AGU 87(36), Ocean Sci. Meet. Suppl., Abstract OS33M-03, (2006)

41. G. C. Pitcher, and D. Calder, "Harmful algal blooms of the southern Benguela current: A review and appraisal of monitoring from 1989 to 1997," S. Afr. J. mar. Sci. 22:255-271, (2000)

42. S. Bernard, C. Balt, G. Pitcher, T. Probyn, A. Fawcett, and A. Du Randt, "The use of MERIS for harmful algal bloom monitoring in the Southern Benguela". Proceedings of the MERIS (A) ATSR Workshop, (2005)

43. J. Gower and S. King, "Intense Plankton Blooms and Sargassum Detection by MERIS," Proceedings of the MERIS and (A) ATSR workshop ESRIN, Frascati, Italy from 26-30 September 2005

44. M. He, Y. Wang, L. Hu, Q. Yang, S. He, C. Hu, and R. Doerffer, "Detection of red tides using MERIS 681 nm and 709 nm bands in the East China Sea: A case study", Proc. Dragon 1 Programme Final Results 2004-2007, Beijing, P. R. China 21-25 April 2008 (ESA SP-655, April 2008)

45. Y. Q. Chen, and X.Q. Shen, "Changes in the Biomass of the East China Sea Ecosystem," In Kenneth Sherman and Qisheng Tang (eds), Large Marine Ecosystems

of the Pacific Rim-Assessment, Sustainability, and Management. (Blackwell Science) pp. 221-239, (1999)

46. R. Amin, J. Zhou, A. Gilerson, B. Gross, F. Moshary and S. Ahmed, "Detection of *Karenia brevis* harmful algal blooms in the West Florida Shelf using red bands of MERIS imagery," OCEANS 08 MTS/IEEE Quebec, Canada, September 15-18, (2008)

Bibliography

CHAPTER 1

1. Red Tide in Texas – An Explanation of the Phenomenon. Bulletin TAMU-G-86-006 C2. Marine Information Service, Sea Grant College Program, Texas A&M University, College Station, Texas. (1986)

2. G. M. Hallegraeff, In G. M. Hallegraeff, D. M. Anderson, and A. D. Cembella [eds.], Manual on harmful marine microalgae, UNESCO, (2003)

3. P. M. Glibert, D. M. Anderson, P. Gentien, E. Graneli, and K. G. Sellner, The global, complex phenomena of harmful algal blooms. Oceanography 18: 136–147, (2005)

4. A. J. McComb, Eutrophic Shallow Estuaries and Lagoons, 240 pp., CRC Press, Boca Raton, Fla. (1995)

5. T. J. Smayda, Novel and nuisance phytoplankton bloom in the sea: Evidence for global epidemic, in Toxic Marine Phytoplankton: Proceedings of the Fourth International Conference on Toxic Marine Phytoplankton, Held June 26 – 30 in Lund, Sweden, edited by E. Graneli et al., pp. 29–40, Elsevier Sci., New York, (1990)

6. J. H. Landsberg, The effects of harmful algal blooms on aquatic organisms. Reviews in Fisheries Science 10(2): 113-390, (2002)

7. T. J. Smayda, Turbulence, watermass stratification and harmful algal blooms: An alternative view and frontal zones as pelagic seed banks, Harmful algae 1:95-112, (2002)

8. C. V. Hoek, D. G. Mann and H. M. Jahns, Algae. *An introduction to phycology*, Cambridge University Press: 627pp. (1995)

9. S. Rodriguez, A. Coute, L. Tenhage and G. Mascarell, Peridiniopsis durandi sp. nova (Dinophyta), une nouvelle Dinophycee d'eau douce responsible de marees rouge, Algological Studies, 95: 15-29. (1999)

10. A. Sournia, Red-tide and toxic marine phytoplankton of the world ocean: An inquiry into biodiversity, in *Harmful Marine Algal Blooms*, edited by P. Lassus et al., pp. 103-112, Lavoisier, Paris. (1995)

11. T. J. Smayda, Harmful algal blooms: Their ecophysiology and general relevance to phytoplankton blooms in the sea, Limnol. Oceanogr., 42, 1137-1153, (1997)

12. S. C. Gallegos, X. Chen, and M. M. Crawford, A Report to TEXAS PARKS AND WILDLIFE, Remote Sensing Studies of the Gulf of Mexico – an effort in red tide detection, (September 2001)

CHAPTER 2

1. http://www.floridaconservation.org/

2. J. H. Landsberg, and K. A. Steidinger, "A historical review of *Gymnodium breve* red tides implicated in mass mortalities of the manatee (*Trichechus manatus latiriostris*) in Florida, USA," In: Reguera, B., Blanco, J., Fernandez, M.L., Wyatt, T. (Eds.), Proceedings of the 8th International Conference on Harmful Algal Blooms, Vigo, Spain, pp. 97-100, (1998)

3. W. H. Hemmert, "The public health implications of *Gymnodinium breve* red tides, A review of the literature and recent events" In: LoCicero, V.R. (Eds.), Proceedings of the First International Conference on Toxic Dinoflagellate Blooms, pp. 489-497, (1975)

4. S. Asai, J. J. Krzanowski, W. H. Anderson, D. F. Martin, J. B. Polson, R. F. Lockey, S. C. Bukantz, and A. Szentivanyi, "Effects of the toxin of red tide, *Ptychodiscus brevis*, on cannie tracheal smooth muscle: a possible new asthma-triggering mechanism," J. Allerg. Clinic. Immunol. 69, 418-428, (1982)

5. J. P. Cannizzaro, K. L. Carder, F. R. Chen, C. A. Heil, and G. A. Vargo, "A novel technique for detection of the toxic dinoflagellate *Karenia brevis* in the Gulf of Mexico from remotely sensed ocean color data," Continent. Shel. Res. 28, 137-158, (2008)

6. K. L. Mahoney, "Backscattering of light by *Karenia brevis* and implications for optical detection and monitoring," PhD dissertation, Univ. of South. Miss., Stennis Space Cent. (2003)

7. K. L. Carder, R. G. Steward, "A remote-sensing reflectance model of a red-tide dinoflagellate off west Florida," Limnol. Oceanogr. 30, 286-298, (1985)

8. O. Schofield, J. Kerfoot, K. Mahoney, M. Moline, M. Oliver, S. Lohrenz, and G. Kirkpatrick, "Vertical migration of the toxic dinoflagellate *Karenia brevis* and the impact on ocean optical properties," J. Geophys. Res., 111, (2006)

9. G. J. Kirkpatrick, D. F. Millie, M. A. Moline, O. Schofield, "Optical discrimination of a phytoplankton species in natural mixed populations," Limnol. Oceanogr. 45, 467-4718, (2000)

10. D. F. Millie, G. J. Kirkpatrick, B. T. Vinyard, "Relating photosynthetic pigments and in vivo optical density spectra to irradiance for the Florida red-tide dinoflagellate *Gymnodinium breve*," Marine Ecology Progress Series 120, 65-75, (1995)

11. D. F. Millie, O. M. Schofield, G. J. Kirkpatrick, G. Johnsen, P. A. Tester, B. T. Vinyard, "Detection of harmful algal blooms using photopigments and absorption signatures: a case study of the Florida red tide dinoflagellate, *Gymnodinium breve*," Limnol. Oceanogr. 42, 1240-1251, (1997)

12. S. E. Lohrenz, G. L. Fahnenstiel, G. J. Kirkpatrick, C. L. Carroll, K. A. Kelly, "Microphotometric assessment of spectral absorption and its potential application for characterization of harmful algal species," Journal of Phycology 35, 1438-1446, (1999)

13. A. Morel, and Y. Ahn, "Optics of heterotrophic nanoflagellates and ciliates: A tentative assessment of their scattering role in oceanic waters compared to those of bacteria and algal cells," J. Mar: Res. 49, 177-202, (1991)

14. D. Stramski, and D. A. Kiefer, "Light scattering in microorganisms in the open ocean," Prog. Oceanogr. 28, 343-383, (1991)

15. O. Ulloa, S. Sathyendranath, and T. Platt, "Effect of the particle-size distribution on the backscattering ratio in seawater," Appl. Opt. 33, 7070-7077, (1994)

16. M. S. Twardowski, E. Boss, J. B. Macdonald, W. S. Pegau, A. H. Barnard, and J. R. V. Zaneveld, "A model for estimating bulk refractive index from the optical backscattering ratio and the implications for understanding particle composition in case I and case II waters," J. Geophys. Res. 106, 14129-14142, (2001)

17. R. P. Stumpf, M. E. Culver, P. A. Tester, M. Tomlinson, G. J. Kirkpatrick, B. A. Pederson, E. Truby, V. Ransibrahmanakul, and M. Soracco, "Monitoring *Karenia brevis* blooms in the Gulf of Mexico using satellite ocean color imagery and other data," Harmful Algae 2, 147-160, (2003)

18. J. E. O'Reilly, S. Maritorena, D. Siegel, M. C. O'Brien, D. Toole, B. G., Mitchell, et al., "Ocean color chlorophyll a algorithms for SeaWiFS, OC2, and OC4: version 4," In: Hooker, S. B. & Firestone, E. R. (Eds.), *SeaWiFS Postlaunch Calibration and Validation Analyses, Part 3 SeaWiFS Postlaunch Technical Report Series*, (pp. 9-23) Greenbelt, Maryland: NASA, Goddard Space Flight Center (2000)

19. H. R. Gordon, D. K. Clark, J. W. Brown, O. B. Brown, R. H. Evans, W. W. Broenkow, "Phytoplankton pigment concentrations in the Middle Atlantic Bight: comparison of ship determinations and CZCS estimates," Appl. Opt. 22, 20-36, (1983)

20. K. L. Carder, F. R. Chen, Z. P. Lee, S. K. Hawes, D. Kamykowski, "Semi-analytic moderate-resolution imaging spectrometer algorithms for chlorophyll a and absorption with bio-optical domains based on nitrate-depletion temperatures," J. Geophy. Res. 104, 5403-5422, (1999)

21. C. Hu, F. E. Muller-Karger, C. Taylor, K. L. Carder, C. Kelble, E. Johns, and C. A. Heil, "Red tide detection and tracing using MODIS fluorescence data: A regional example in SW Florida coastal waters," Remote Sens. Environ. 97, 311-321, (2005)

22. A. Gilerson, J. Zhou, S. Hlaing, I. Ioannou, R. Amin, B. Gross, F. Moshary, and S. Ahmed, "Fluorescence contribution to reflelctance spectra for a variety of coastal waters," Proc. Of SPIE 6680 (2007)

23. A. Gilerson, J. Zhou, S. Hlaing, I. Ioannou, J. Schalles, B. Gross, F. Moshary, and S. Ahemd, "Fluorescence component in the reflectance spectra from coastal waters. Dependence on water composition," Opt. Express, 15, 15702-15721 (2007)

24. A. Gilerson, J. Zhou, S. Hlaing, I. Ioannou, B. Gross, F. Moshary, and S. Ahmed, "Fluorescence component in the reflectance spectra from coastal waters. II. Performance of retrieval algorithms," Opt. Express 16, 2446-2460, (2008)

25. R. Amin, J. Zhou, A. Gilerson, B. Gross, F. Moshary, and S. Ahmed, " Detection of *Karenia brevis* harmful algal blooms in the West Florida Shelf using red bands of MERIS Imagery," OCEANS 08 MTS/IEEE Quebec, Canada, 15-18 Sept. (2008)

26. http://oceancolor.gsfc.nasa.gov

27. H. R. Gordon, and M. Wang, "Retrieval of water-leaving radiance and aerosol optical thickness over the oceans with SeaWiFS: a preliminary algorithm," Appl. Opt. 33, 443-452 (1994)

28. M. Wang, and W. Shi, "Estimation of ocean contribution at MODIS near infrared wavelengths along the east coast of the U.S.: two case studies," Geophys. Res. Lett. 32, L13606, doi: 10.1029/2005GL022917,(2005)

29. Z. P. Lee, K. L. Carder, C. D. Mobley, R. G. Steward, and J. S. Patch, "Hyperspectral remote sensing for shallow waters: I. A semi-analytical model," Appl. Opt. 37, 6329-6338, (1998)

30. Z. P. Lee, K. L. Carder, C. D. Mobley, R. G. Steward, and J. S. Patch, "Hyperspectral remote sensing for shallow waters: 2. Deriving bottom depths and water properties by optimization" Appl. Opt. 38, 3831-3843, (1999)

31. R. Pope, and E. Fry, "Absorption spectrum (380 – 700 nm) of pure waters: II. Integrating cavity measurements" Appl. Opt. 36, 8710-8723, (1997)

32. Z. P. Lee, http://www.ioccg.org/groups/OCAG_data.html

33. A. Morel, "Optical properties of pure water and pure seawater," in *Optical Aspects of Oceanography,* N. G. Jerlov and E. S. Nielsen, eds., (Academic, New York, 1974)

34. Z. P. Lee, and K. L. Carder, "Band-ratio of spectral-curvature algorithms for satellite remote sensing?" Appl. Opt. 39, 4377-4380, (2000)

35. T. J. Smayda, "Harmful algal blooms: their ecophysology and general relevance to phytoplankton blooms in the sea," Limnol. Oceanogr. 42, 1137-1153, (1997)

36. D. Stramski, A. Bricaud, and A. Morel, "Modeling the Inherent Optical Properties of the Ocean Based on the Detailed Composition of the Planktonic Community," Appl. Opt. 40, 2929-2945 (2001)

37. C. S. Roesler, and E. Boss, "Spectral beam attenuation coefficient in the ocean color inversion" Geophys. Res. Lett. 30, 1468, doi:10.1029/2002GL016185 (2003)

38. Y. Huot, C. A. Brown, and J. J. Cullen, "New algorithms for MODIS sun-induced chlorophyll fluorescence and a comparison with present data products" Limnol. Oceanogr. Methods 3, 108-130, (2005)

39. J. Zhou, A. Gilerson, I. Ioannou, S. Hlaing, J. Schalles, B. Gross, F. Moshary, and S. Ahmed, "Retrieving quantum yield of sun-induced chlorophyll fluorescence near surface from hyperspectral in-situ measurement in productive water," Opt. Express 16, 17468-17483 (2008)

40. W. W. Gregg, and K. L. Carder, "A simple spectral solar irradiance model for cloudless maritime atmospheres," Limnol. Oceanogr. 35, 1657-1675, (1990)

41. A. Albert, and C. D. Mobely, "An analytical model for subsurface irradiance and remote sensing reflectance in deep and shallow case-2 waters," Opt. Express 11, 2873-2890, (2003)

42. A. Morel, and S. Maritorena, "Bio-optical properties of ocean waters: A reappraisal" J. Geophys.l Res. 106, 7163-7180, (2001)

43. http://oceancolor.gsfc.nasa.gov/DOCS/MSL12/master_prodlist.html/#nLw

44. J. J. Walsh, J. K. Jolliff, B. P. Darrow, J. M. Lenes, S. P. Milroy, A. Remsen, D. A. Dieterle, K. L. Carder etc., "Red tides in the Gulf of Mexico: where, when, and why?" J. Geophy. Res. 111, C11003, (2006)

45. K. L. Carder, J. P. Cannizzaro, F. R. Chen, C. Hu, " Detecting HAB's in the Gulf of Mexico: Problems with atmospheric correction and shallow waters," MODIS Science Team Meeting, (2005)

46. FWRI, http://www.floridamarine.org

47. R. Amin, A. Gilerson, J. Zhou, B. Gross, F. Moshary, and S. Ahmed, " Impacts of atmospheric corrections on algal bloom detection techniques," 89th AMS Annual Meeting, Phoenix, Arizona, 11-15 Jan, (2009)

48. M. C. Tomlinson, R. P. Stumpf, V. Ransibrahmanakul, E. W. Truby, G. J. Kirkpatrick, B. A. Pederson, G. A. Vargo, C. A. Heil, "Evaluation of the use of SeaWiFS imagery for detecting *Karenia brevis* harmful algal blooms in the eastern Gulf of Mexico," Remote Sens. Environ. 91, 293-303, (2004)

49. http://www.nasa.gov/centers/goddard/news/topstory/2004/0826planktonglow.html

50. http://nasascience.nasa.gov/earth-science/applied-sciences/national-applications/coastal-managment

51. http://coastwatch.noaa.gov/hab/bulletins_ns.htm

52. C. Hu, F. E. Muller-Karger, and P. W. Swarzenski, "Hurricanes, submarine groundwater discharge, and Florida's red tides," Geophys. Res. Lett. 33, L11601, doi: 10.1029/2005GL025449, (2006)

53. http://www.tpwd.state.tx.us/landwater/water/environconcerns/hab/redtide/status.phtml

54. A. Subramaniam, E. J. Carpenter, and P. G. Falkowski, "Bio-optical properties of the marine diazotrophic cyanobacteria *Trichodesmium spp*. II. A reflectance model for remote sensing," Limnol. Oceanogr. 44, 618-627, (1999)

55. D. MacKee, A. Cunningham, D. Wright, and L. Hay, "Potential impacts of nonalgal materials on water-leaving Sun induced chlorophyll fluorescence signals in coastal waters," Appl. Opt. 46, 7720-7729, (2007)

56. M. C. Tomlinson, T. T. Wynne, and R. P. Stumpf, "An evaluation of remote sensing techniques for enhanced detection of the toxic dinoflagellate, *Karenia brevis*," Remote Sens. Environ., doi:10.1016/j.rse.2008.11.003, (2008)

57. C. Hu, Z. P. Lee, F. E. Muller-Karger, and K. L. Carder, "Application of an optimization algorithm to satellite ocean color imagery: A case study in Southwest Florida coastal waters," In J. Frouin, Y. Yuan, & H. Kawamura (Eds.) SPIE Proceedings. *Ocean Remote Sensing and Applications*, vol. 4892 (pp. 70-79). Bellingham, WA: SPIE, (2003)

CHAPTER 3

1. H. R. Gordon, and M. Wang, "Retrieval of water-leaving radiance and aerosol optical thickness over the oceans with SeaWiFS: a preliminary algorithm," Appl. Opt. 33, 443-452 (1994)

2. M. Wang, and W. Shi, "Estimation of ocean contribution at MODIS near infrared wavelengths along the east coast of the U.S.: two case studies," Geophys. Res. Lett. 32, L13606, doi: 10.1029/2005GL022917,(2005)

3. R. Amin, A. Gilerson, J. Zhou, B. Gross, F. Moshary, and S. Ahmed, " Impacts of atmospheric corrections on algal bloom detection techniques," 89th AMS Annual Meeting, Phoenix, Arizona, 11-15 Jan, (2009)

4. D. A. Siegel, M. Wang, S. Maritorena, W. Robinson, "Atmospheric correction of satellite ocean color imagery: the black pixel assumption," Appl. Opt. 39, 3582-3591, (2000)

5. C. Hu, K. L. Carder, F. E. Muller-Karger, "Atmospheric correction of SeaWiFS imagery over turbid coastal waters: a practical method," Remote Sens. Environ. 74, 195-206, (2000)

6. C. Hu, F. E. Muller-Karger, C. Taylor, K. L. Carder, C. Kelble, E. Johns, and C. A. Heil, "Red tide detection and tracing using MODIS fluorescence data: A regional example in SW Florida coastal waters," Remote Sens. Environ. 97, 311-321, (2005)

7. R. Amin, J. Zhou, A. Gilerson, B. Gross, F. Moshary, and S. Ahmed, " Detection of *Karenia brevis* harmful algal blooms in the West Florida Shelf using red bands of MERIS Imagery," OCEANS 08 MTS/IEEE Quebec, Canada, 15-18 Sept. (2008)

8. R. Amin, J. Zhou, A. Gilerson, B. Gross, F. Moshary and S. Ahmed, "Use of MODIS Ocean Color Imagery for Improved Detection and Monitoring of *Karenia brevis* Blooms in the Gulf of Mexico," Ocean Optics XIX Tuscany, Italy, October 6-10, 2008

CHAPTER 4

1. A. J. McComb, (Ed.), "Eutrophic Shallow Estuaries and Lagoons," 240 pp., CRC Press, Boca Raton, Fla. (1995)

2. T. J. Smayda, "Novel and nuisance phytoplankton bloom in the sea: Evidence for global epidemic," in Toxic Marine Phytoplankton: Proceedings of the Fourth International Conference on Toxic Marine Phytoplankton, Held June 26 – 30 in Lund, Sweden, edited by E. Graneli et al., pp. 29–40, Elsevier Sci., New York, (1990)

3. P. Hoagland, and S. Scatasta, "The economic effects of harmful algal blooms," In E. Graneli and J. Turner, eds., Ecology of Harmful Algae. Ecology Studies Series. Dordrecht, The Netherlands: Springer-Verlag, Chap. 29, (2006)

4. C. V. Hoek, D. G. Mann and H. M. Jahns, "Algae. *An introduction to phycology*," Cambridge University Press: 627pp. (1995)

5. S. Rodriguez, A. Coute, L. Tenhage and G. Mascarell, "Peridiniopsis durandi sp. nova (Dinophyta), une nouvelle Dinophycee d'eau douce responsible de marees rouge," Algological Studies, 95: 15-29. (1999)

6. A. Sournia, "Red-tide and toxic marine phytoplankton of the world ocean: An inquiry into biodiversity," in *Harmful Marine Algal Blooms*, edited by P. Lassus et al., pp. 103-112, Lavoisier, Paris. (1995)

7. T. J. Smayda, “Harmful algal blooms: Their ecophysiology and general relevance to phytoplankton blooms in the sea,” Limnol. Oceanogr., 42, 1137-1153, (1997)

8. T. J. Smayda, “Turbulence, watermass stratification and harmful algal blooms: An alternative view and frontal zones as pelagic seed banks,” Harmful algae 1:95-112, (2002)

9. J. H. Ryther, “Ecology of autotrophic marine dinoflagellates with reference to red water condition,” pp. 387-414 in The *Luminescence of Biological Systems*, F. H. Johnson, ed. American Association for the Advancement of Science, Washington, D.C. USA. (1955)

10. R. Margalef, M. Estrada, and D. Blasco, “Functional morphology of organisms involved in red tides, as adapted to decaying turbulence,” pp. 89-94 in Toxic Dinoflagellate Blooms, Proceedings of the Second International Conference on toxic dinoflagellate blooms. D. L. Taylor and H. H. Seliger, eds. Elsevier, New York, NY. USA. (1979)

11. J. J. Cullen, and S. G. Horrigan, “Effects of nitrate on the diurnal vertical migration, carbon to nitrogen ratio, and the photosynthetic capacity of the dinoflagellate Gymnodinium splendens,” *Mar. Biol. Berlin*, 62, 81-89. (1981)

12. S. I. Heaney, and R. W. Eppley, “Light, temperature and nitrogen as interacting factors affecting diel vertical migrations of dinoflagellates in culture,” *J. Plankton Res., 3*(2), 331-344. (1981)

13. A. Morel, and Y. Ahn, “Optics of heterotrophic nanoflagellates and ciliates: A tentative assessment of their scattering role in oceanic waters compared to those of bacteria and algal cells,” J. Mar: Res. 49, 177-202, (1991)

14. D. Stramski, and D. A. Kiefer, “Light scattering in microorganisms in the open ocean,” Prog. Oceanogr. 28, 343-383, (1991)

15. E. J. Buskey, P. A. Montagna, A. F. Amos, and T. E. Whitledge, “Disruption of grazer populations as a contributing factor to the initiation of the Texas brown tide algal bloom”, Limnol. Oceanogr., 42, 1215-1222 (1997)

16. O. Schofield, J. Kerfoot, K. Mahoney, M. Moline, M. Oliver, S. Lohrenz, and G. Kirkpatrick, “Vertical migration of the toxic dinoflagellate *Karenia brevis* and the impact on ocean optical properties,” J. Geophys. Res., 111, (2006)

17. J. P. Cannizzaro, K. L. Carder, F. R. Chen, C. A. Heil, and G. A. Vargo, “A novel technique for detection of the toxic dinoflagellate *Karenia brevis* in the Gulf of Mexico from remotely sensed ocean color data,” Continent. Shel. Res. 28, 137-158, (2008)

18. Z. P. Lee, http://www.ioccg.org/groups/OCAG_data.html

19. R. P. Stumpf, M. E. Culver, P. A. Tester, M. Tomlinson, G. J. Kirkpatrick, B. A. Pederson, E. Truby, V. Ransibrahmanakul, and M. Soracco, "Monitoring *Karenia brevis* blooms in the Gulf of Mexico using satellite ocean color imagery and other data," Harmful Algae 2, 147-160, (2003)

20. R. Amin, J. Zhou, A. Gilerson, B. Gross, F. Moshary and S. Ahmed, "Novel Optical Techniques for Detecting and Classifying Toxic Dinoflagellate *Karenia brevis* Blooms Using Satellite Imagery," Optics Express Vol. 17, Iss. 11, pp. 9126-9144 (2009)

21. R. Amin, A. Gilerson, J. Zhou, B. Gross, F. Moshary and S. Ahmed, "Impacts of Atmospheric Corrections on Algal Bloom Detection Techniques," 89th AMS Annual Meeting, Phoenix, Arizona, January 11-15, (2008)

22. R. Amin, J. Zhou, A. Gilerson, B. Gross, F. Moshary and S. Ahmed, "Use of MODIS Ocean Color Imagery for Improved Detection and Monitoring of *Karenia brevis* Blooms in the Gulf of Mexico," Ocean Optics XIX Tuscany, Italy, October 6-10, (2008)

23. J. Gower, S. King, G. Borstad, and L. Brown, "Detection of intense plankton blooms using the 709nm band of the MERIS imaging spectrometer," *Int. J. Remote Sens*., 26, 2005-2012. (2005)

24. http://merci-srv.eo.esa.int/merci/welcome.do

25. http://oceancolor.gsfc.nasa.gov

26. H. R. Gordon, and M. Wang, "Retrieval of water-leaving radiance and aerosol optical thickness over the oceans with SeaWiFS: a preliminary algorithm," Appl. Opt. 33, 443-452 (1994)

27. http://www.floridaconservation.org/

28. J. H. Landsberg, and K. A. Steidinger, "A historical review of *Gymnodium breve* red tides implicated in mass mortalities of the manatee (*Trichechus manatus latiriostris*) in Florida, USA," In: Reguera, B., Blanco, J., Fernandez, M.L., Wyatt, T. (Eds.), Proceedings of the 8th International Conference on Harmful Algal Blooms, Vigo, Spain, pp. 97-100, (1998)

29. W. H. Hemmert, "The public health implications of *Gymnodinium breve* red tides, A review of the literature and recent events" In: LoCicero, V.R. (Eds.), Proceedings of the First International Conference on Toxic Dinoflagellate Blooms, pp. 489-497, (1975)

30. S. Asai, J. J. Krzanowski, W. H. Anderson, D. F. Martin, J. B. Polson, R. F. Lockey, S. C. Bukantz, and A. Szentivanyi, "Effects of the toxin of red tide, *Ptychodiscus brevis*, on cannie tracheal smooth muscle: a possible new asthma-triggering mechanism," J. Allerg. Clinic. Immunol. 69, 418-428, (1982)

31. K. L. Carder, J. P. Cannizzaro, F. R. Chen, C. Hu, " Detecting HAB's in the Gulf of Mexico: Problems with atmospheric correction and shallow waters," MODIS Science Team Meeting, (2005)

32. http://www.tpwd.state.tx.us/landwater/water/environconcerns/hab/redtide/status.phtml

33. C. Hu, F. E. Muller-Karger, C. Taylor, K. L. Carder, C. Kelble, E. Johns, and C. A. Heil, "Red tide detection and tracing using MODIS fluorescence data: A regional example in SW Florida coastal waters," Remote Sens. Environ. 97, 311-321, (2005)

34. FWRI, http://www.floridamarine.org

35. J. P. Ryan, J. F. R. Gower, S. A. King, W. P. Bissett, A. M. Fischer, R. M. Kudela, Z. Kolber, F. Mazzillo, E. V. Rienecker, and F. P. Chavez, "A coastal ocean extreme bloom incubator", Geophysical Research Lett, Vol 35, L12602, (2008)

36. J. P. Ryan, H. M. Dierssen, R. M. Kudela, C. A. Scholin, K. S. Johnson, J. M. Sullivan, A. M. Fischer, E. V. Rienecker, P. R. McEnaney, and F. P. Chavez, "Coastal ocean physics and red tides: An example from Monterey Bay, California," Oceanography 18, 246-255. (2005)

37. R. M. Kudela, J. P. Ryan, M. D. Blakely, J. Q. Lane and T. D. Peterson, "Linking the physiology and ecology of Cochlodinium to better understand harmful algal bloom events: A comparative approach," Harmful Algae, 7, 278-292 (2008)

38. D. Blasco, "Observations on the diel migration of marine dinoflagellates off the Baja California coast," Mar. Biol. Berlin, 46, 41-47. (1978)

39. J. G. Park, M. K. Jeong, J. A. Lee, K. J. Cho, and O. S. Kwon, "Diurnal vertical migration of a harmful dinoflagellate, Cochlodinium polykrikoides (Dinophyceae), during a red tide in coastal waters of Namhae Island, Korea," Phycologia, 40, 292-297. (2001)

40. P. L. Donaghay, J. M. Sullivan, J. E. Rines, J. Graff, A. K. Hanson, and D. V. Holliday, "The importance of swimming behavior in controlling the formation, maintenance and dissipation of thin optical layers," Eos Trans. AGU 87(36), Ocean Sci. Meet. Suppl., Abstract OS33M-03, (2006)

41. G. C. Pitcher, and D. Calder, “Harmful algal blooms of the southern Benguela current: A review and appraisal of monitoring from 1989 to 1997,” S. Afr. J. mar. Sci. 22:255-271, (2000)

42. S. Bernard, C. Balt, G. Pitcher, T. Probyn, A. Fawcett, and A. Du Randt, “The use of MERIS for harmful algal bloom monitoring in the Southern Benguela”. Proceedings of the MERIS (A) ATSR Workshop, (2005)

43. J. Gower and S. King, “Intense Plankton Blooms and Sargassum Detection by MERIS,” Proceedings of the MERIS and (A) ATSR workshop ESRIN, Frascati, Italy from 26-30 September 2005

44. M. He, Y. Wang, L. Hu, Q. Yang, S. He, C. Hu, and R. Doerffer, “Detection of red tides using MERIS 681 nm and 709 nm bands in the East China Sea: A case study”, Proc. Dragon 1 Programme Final Results 2004-2007, Beijing, P. R. China 21-25 April 2008 (ESA SP-655, April 2008)

45. Y. Q. Chen, and X.Q. Shen, “Changes in the Biomass of the East China Sea Ecosystem,” In Kenneth Sherman and Qisheng Tang (eds), Large Marine Ecosystems of the Pacific Rim-Assessment, Sustainability, and Management. (Blackwell Science) pp. 221-239, (1999)

46. R. Amin, J. Zhou, A. Gilerson, B. Gross, F. Moshary and S. Ahmed, “Detection of *Karenia brevis* harmful algal blooms in the West Florida Shelf using red bands of MERIS imagery,” OCEANS 08 MTS/IEEE Quebec, Canada, September 15-18, (2008)

PUBLICATIONS AND PRESENTATIONS

1. **R. Amin**, J. Zhou, A. Gilerson, B. Gross, F. Moshary and S. Ahmed, "Novel Optical Techniques for Detecting and Classifying Toxic Dinoflagellate *Karenia brevis* Blooms Using Satellite Imagery," Optics Express Vol. 17, Iss. 11, pp. 9126-9144 (2009)

2. **R. Amin**, A. Gilerson, B. Gross, F. Moshary, and S. Ahmed, "MODIS and MERIS Detection of Dinoflagellates Blooms using the RBD Technique," SPIE Europe Remote Sensing, Berlin, Germany, August 31- September 3, 2009

3. **R. Amin**, "Planktons Gone Wild: Hunting Toxic Planktons from Space," 6th Annual NOAA/NESDIS/STAR/CoRP Symposium, The City College of the City University of New York, August 18-19, 2009

4. **R. Amin,** A. Gilerson, R. Gould, R. Arnone, and S. Ahmed, "Extreme Algal Blooms Detection with MERIS," AGU 2009 Joint Assembly Meeting, Toronto, Ontario, Canada, May 24-27, 2009

5. **R. Amin**, "Algorithms for Toxic Algal Blooms Detection," 8th Annual NOAA-CREST Advisory and Scientific Board Meeting, UMBC, Baltimore, MD, May 7-8, 2009

6. S. Ahmed, A. Gilerson, J. Zhou, **R. Amin**, R. Dyer, B. Gross, F. Moshary, "NIR Reflectance and its Application to Fluorescence, Chlorophyll and Algal Bloom Coastal Water Retrievals," ASLO Aquatic Sciences Meeting, Nice, France, January 25-30, 2009

7. **R. Amin**, A. Gilerson, J. Zhou, B. Gross, F. Moshary and S. Ahmed, "Impacts of Atmospheric Corrections on Algal Bloom Detection Techniques," 89th AMS Annual Meeting, Phoenix, Arizona, January 11-15, 2008

8. **R. Amin**, J. Zhou, A. Gilerson, B. Gross, F. Moshary and S. Ahmed, "Comparison of Techniques for Satellite Detection of Red Tides in the Gulf of Mexico," AGU Fall Meeting, San Francisco, December 15-19, 2008

9. **R. Amin**, "Optical Detection and Classification of *Karenia* off the West Coast of Florida from Remotely Sensed Ocean Color Data," Naval Research Laboratory, Stennis Space Center, MS, November 14, 2008

10. **R. Amin**, J. Zhou, A. Gilerson, B. Gross, F. Moshary and S. Ahmed, "Use of MODIS Ocean Color Imagery for Improved Detection and Monitoring of *Karenia brevis* Blooms in the Gulf of Mexico," Ocean Optics XIX Tuscany, Italy, October 6-10, 2008

11. **R. Amin**, J. Zhou, A. Gilerson, B. Gross, F. Moshary and S. Ahmed, "Detection of *Karenia brevis* harmful algal blooms in the West Florida Shelf using red bands of MERIS imagery," OCEANS 08 MTS/IEEE Quebec, Canada, September 15-18, 2008

12. **R. Amin**, J. Zhou, A. Gilerson, B. Gross, F. Moshary and S. Ahmed, "Optical classification of red tide organism *Karenia brevis* in the coastal waters of the Gulf of Mexico," 5th Annual CoRP Science Symposium, Corvallis, Oregon, August 12-13, 2008

13. N. Steiner, I. Ioannou, **R. Amin, J.** Zhou, A. Gilerson, B. Gross, F. Moshary, and S. Ahmed, "Characteristics of CDOM absorption in UV and their application for the advanced IOP retrieval algorithms," 2008 Ocean Sciences Meeting, Orlando, Florida, March 2-7, 2008

14. **R. Amin**, A. Gilerson, B. Gross, F. Moshary and S. Ahmed, "Detecting Harmful Algal Blooms with satellite ocean color imagery in the coastal waters," 6th Annual NOAA-CREST Symposium Mayaguez, Puerto Rico, February 20-22, 2008

15. A. Gilerson, J. Zhou, S. Hlaing, I. Ioannou, **R. Amin**, B. Gross, F. Moshary, S. Ahmed, "Fluorescence contribution to reflectance spectra for a variety of coastal waters," Proc. of SPIE 6680, San Diego, CA, August, 2007

16. **R. Amin**, J. Zhou, A. Gilerson, B. Gross, F. Moshary and S. Ahmed, "Evaluation of IOPs accuracy measurements and its impact on simulated reflectances," The Fourth Annual NOAA/NESDIS/StAR/CoRP Symposium, College Park, Maryland, June 19-20, 2007

17. S. Ahmed, A. Gilerson, J. Zhou, J. Chowdhary, I. Ioannou, **R. Amin**, B. Gross, F. Moshary. Evaluation of the impact of backscatter spectral characteristics on Chl retrievals in coastal waters. Proc. SPIE Vol. 6406, 64060A, Remote Sensing of the Marine Environment; Robert J. Frouin, Vijay K. Agarwal, Hiroshi Kawamura, Shailesh Nayak, Delu Pan; Eds. Goa, India, November, 2006

18. **R. Amin**, I. Ioannou, T. Iijima, S. Hliang, J. Zhou, A. Gilerson, B. Gross, F. Moshary and S. Ahmed, "Comparison of measured and simulated reflectances in the coastal waters," Fourth NOAA-EEP Conference, Tallahassee, Florida, October 30 to November 1, 2006

19. **R. Amin,** R. Fortich, J. Zhou, A. Gilerson, B. Gross, F. Moshary and S. Ahmed. "Variability of the Inherent Optical Properties in the waters of Chesapeake Bay and Eastern Long Island" Fourth Annual NOAA-CREST Symposium Mayaguez, Puerto Rico, February 23-25, 2006